Strong postmating reproductive isolation in *Mimulus* section *Eunanus*

Matthew C. Farnitano[1]*, Andrea L. Sweigart[1]

[1]Department of Genetics, University of Georgia, Athens, GA, 30602, USA.

*Corresponding author:

Matthew C. Farnitano

120 W. Green St

Athens, GA 30602

mattfarnitano@gmail.com

ABSTRACT

Postmating reproductive isolation can help maintain species boundaries when premating barriers to reproduction are incomplete. The strength and identity of postmating reproductive barriers are highly variable among diverging species, leading to questions about their genetic basis and evolutionary drivers. These questions have been tackled in model systems but are less often addressed with broader phylogenetic resolution. In this study we analyze patterns of genetic divergence alongside direct measures of postmating reproductive barriers in an overlooked group of sympatric species within the model monkeyflower genus, *Mimulus*. Within this *Mimulus brevipes* species group, we find substantial divergence among species, including a cryptic genetic lineage. However, rampant gene discordance and ancient signals of introgression suggest a complex history of divergence. In addition, we find multiple strong postmating barriers, including postmating prezygotic isolation, hybrid seed inviability, and hybrid male sterility, leading to complete or substantial postmating isolation in all species pairs. Hybrid seed inviability appears linked to differences in seed size, providing a window into possible developmental mechanisms underlying this reproductive barrier. While geographic proximity and incomplete mating isolation may have allowed gene flow within this group in the distant past, strong postmating reproductive barriers today are likely to prevent any ongoing hybridization. By producing foundational information about reproductive isolation and genomic divergence in this understudied group, we add new diversity and phylogenetic resolution to our understanding of the mechanisms of plant speciation.

KEY WORDS: postmating reproductive isolation, introgression, *Mimulus*, hybrid seed inviability, speciation

INTRODUCTION

Evolutionary biologists have long been interested in understanding what patterns and processes lead to reproductive isolation among species (Coyne & Orr, 1997; Darwin, 1859; V. Grant, 1981). Reproductive isolation is often broken down into components that act at sequential stages of the life cycle – premating barriers such as ecogeographic isolation and pollinator-mediated isolation that prevent mating, postmating prezygotic barriers that reduce fertilization success after mating has occurred, and postmating postzygotic barriers that reduce the fitness of hybrid offspring relative to pure species (Ramsey et al., 2003; Sobel & Chen, 2014). In plants, premating barriers are typically thought to evolve more quickly than postmating barriers and to have a greater contribution to overall isolation (Christie et al., 2022). However, this general pattern masks a great deal of heterogeneity across species pairs: many systems are completely isolated by premating barriers, while others rely exclusively on strong postmating isolation; many have a mix of both. Postmating barriers are often the result of intrinsic genetic incompatibilities, making them potentially more stable over the long term than ecologically mediated premating barriers (Coughlan & Matute, 2020). Postmating barriers may also be a source of cryptic variation in groups without obvious morphological or ecological differences.

To fully understand the role that postmating reproductive barriers play in speciation, they must be placed in a phylogenetic context. The degree of reproductive isolation between two taxa tends to increase with genetic distance (Christie & Strauss, 2018; Coyne & Orr, 1989;

66 Malone & Fontenot, 2008; Scopece et al., 2007), but this relationship is not always consistent
67 across taxa (Moyle et al., 2004) and is highly heterogeneous. In addition, individual
68 reproductive barriers such as sterility and inviability may arise at different rates (Coyne & Orr,
69 1989; Le Gac et al., 2007; Malone & Fontenot, 2008; Presgraves, 2002). The reasons behind
70 these differences are a subject of ongoing investigation, but may include differences in genetic
71 architecture (Guerrero et al., 2017; Moyle & Payseur, 2009) or the forms of selection acting on
72 each barrier (Baack et al., 2015). For example, conflicting selection pressures between maternal
73 and paternal genomes in the mammalian placenta or the flowering plant endosperm are
74 thought to give rise to reproductive barriers as these conflicts are resolved differently in
75 independent lineages (Crespi & Nosil, 2013; Haig & Westoby, 1991; Lafon-Placette & Köhler,
76 2016); the relative strength of this parental conflict could influence the rate of barrier evolution
77 (Coughlan et al., 2020; Raunsgard et al., 2018).
78 An excellent system for building a phylogenetically informed understanding of
79 reproductive isolation is the western North American radiation of monkeyflowers in the genus
80 *Mimulus.* Multiple species groups within *Mimulus* have already been studied extensively in a
81 speciation context, including the *Mimulus guttatus* (e.g., Brandvain et al., 2014; Ferris et al.,
82 2014; Lowry & Willis, 2010), *M. aurantiacus* (e.g., Stankowski et al., 2019; Streisfeld & Kohn,
83 2005), and *M. lewisii* (e.g., Nelson et al., 2021; Ramsey et al., 2003) species complexes. A
84 number of pre- and postmating reproductive barriers have been mapped to single genes or QTL
85 (e.g., Fishman et al., 2014; Fishman & Willis, 2006; Streisfeld & Rausher, 2009; Sweigart et al.,
86 2006; Yuan et al., 2013; Zuellig & Sweigart, 2018). Recently, hybrid seed inviability in particular
87 has been identified as a strong barrier in multiple independent species pairs of the *Mimulus*

88 *guttatus* species complex, with parental conflict repeatedly implicated as a common
89 mechanism (Coughlan et al., 2020; Oneal et al., 2016; Sandstedt et al., 2020; Sandstedt &
90 Sweigart, 2022). An expanding trove of genetic and developmental resources across the genus
91 allow for a holistic approach to understanding reproductive isolation from genic to phylogenetic
92 scales (Yuan, 2019).

93 However, some *Mimulus* subgroups have received less attention, in part because they
94 are less experimentally tractable or more difficult to access. Studies in these other groups
95 would provide an important complement to existing knowledge, facilitating comparative
96 analysis at the genus level while highlighting overlooked diversity in the genetic and ecological
97 mechanisms of speciation. One such neglected group is *Mimulus* section *Eunanus* [synonym
98 *Diplacus* section *Eunanus,* see (Barker et al., 2012; Lowry et al., 2019) for a discussion of
99 nomenclatural issues]. Section *Eunanus* is a clade of ~23 species (A. L. Grant, 1924; Nesom,
100 2013) which prior to this publication has had no genome-scale sequencing and few assessments
101 of reproductive isolation. The group includes both widespread and narrowly endemic species
102 occupying a range of elevations and habitats in western North America. Here, we focus
103 primarily on three species from this group: *Mimulus brevipes* Benth*., Mimulus fremontii*
104 (Benth.) Gray*, and Mimulus johnstonii* Grant (Baldwin et al., 2012; A. L. Grant, 1924). These
105 three morphologically defined species make up a well-supported clade according to a
106 phylogenetic study of *Mimulus* based on three genetic markers (Beardsley et al., 2004). Their
107 ranges are overlapping; *M. johnstonii* is restricted to higher elevations in the Transverse Ranges
108 of southern California, while *M. fremontii* and *M. brevipes* are more widespread throughout the
109 coastal ranges from Monterey into Baja California (Figure 1B).

110 Studies of reproductive isolation in these three species are limited. Species distribution
111 modeling between *Mimulus johnstonii* and *M. brevipes* identified strong but incomplete
112 ecogeographical isolation (RI=0.65 and 0.82 reciprocally) (Sobel, 2014), and they can be found
113 within hundreds of feet of each other (pers. obs.). No distribution models have been made with
114 *M. fremontii*, but M*. brevipes* and *M. fremontii* are found at similar elevations, flower at similar
115 times, and can be found growing within inches of each other (pers. obs.). Major differences in
116 flower color, size, and shape between *M. brevipes* and its relatives might suggest some degree
117 of pollinator-mediated isolation, though little is known about the identity of pollinators or
118 levels of outcrossing; *M. fremontii* and *M. johnstonii* have similar floral characteristics and seem
119 unlikely to have substantial pollinator isolation. Postmating barriers have not been studied,
120 with the exception of one study showing low germination rates of F1 hybrid seeds between *M.*
121 *brevipes* and *M. johnstonii,* potentially suggesting hybrid seed inviability (Sobel, 2010).
122 In this study, we present the first genome-scale analysis of divergence relationships in
123 *Mimulus* section *Eunanus*, incorporating our three focal species as well as two more distant
124 species, *M. constrictus* and *M. nanus*. In addition, we use controlled crosses to examine
125 multiple postmating reproductive barriers between the focal species. We find clear genetic
126 divergence and multiple strong postmating reproductive barriers between all tested species.
127 Our results add to a growing body of evidence that intrinsic postmating barriers, especially
128 hybrid seed inviability, are a key component in the maintenance of plant species.
129

130 **MATERIALS AND METHODS**

131 *Sample collections and growth conditions*

132 Fruits were collected from wild plants of three focal species (*M. brevipes, M. fremontii,*
133 and *M. johnstonii*) at nine locations in southern California in summer 2019 (Figure 1B, Table S1).
134 As additional, more phylogenetically distant comparisons, a population of *M. nanus* in Oregon
135 and a population of *M. constrictus* from California were collected in 2021. To germinate, we
136 treated seeds overnight with 1 mM giberrellic acid, then rinsed three times with distilled water
137 and placed them individually in 2x2cm soil plugs. Soil was a 1:1:1 mix of sand, perlite, and peat
138 with a thin layer of finely sifted soil mix on top. Germination trays were set in standing bottom
139 water and kept moist with a squirt bottle as necessary. When germination rates were low,
140 liquid smoke was added to standing water to simulate post-fire conditions and stimulate
141 germination. After germinants developed one or two pairs of true leaves, we transplanted soil
142 plugs into plastic conical pots filled with the same soil mix. The conical pots were maintained in
143 standing bottom water in a growth chamber set to 23C days/18C nights, with low relative
144 humidity and 16 hours of daylight. Germination and establishment was low overall and highly
145 variable across species, populations, and trials, so germination and establishment rates were
146 not used as a proxy for seed viability or hybrid fitness.
147 One population initially collected as *M. johnstonii,* S25 from Sespe Creek, showed
148 morphological differences suggesting it may be a unique lineage, and is treated separately
149 throughout this paper. Compared to *M. johnstonii*, Sespe Creek has inserted stigmas, a lighter
150 purple corolla with a slight white wash at the mouth, and longer leaf trichomes.
151
152 *Genomic sequencing*

153 We collected leaf tissue from 33 individuals for genomic sequencing. All sequenced
154 individuals were generated from outbred field-collected seeds and germinated in growth
155 chambers. We flash-froze leaf tissue in liquid nitrogen and used a modified CTAB-based
156 protocol to extract genomic DNA (Fishman, 2020). Briefly, tissue was ground to a powder and
157 incubated in CTAB buffer with ß-mercaptoethanol. Supernatant was extracted with phenol-
158 chloroform-isoamyl alcohol, then again with chloroform-isoamyl alcohol, followed by
159 precipitation of carbohydrates with sodium chloride and polyethylene glycol. DNA was then
160 precipitated with isopropanol, washed with ethanol, and resuspended in distilled water.
161 We used the tagmentation-based Illumina Nextera XT DNA library prep kit (FC-131-1024)
162 to prepare genomic DNA for sequencing. The 33 individually barcoded samples were then
163 sequenced in four batches at the Duke University Sequencing and Genomic Technologies
164 Shared Resource with either an Illumina NextSeq 500 or an Illumina NovaSeq 6000 sequencer,
165 in combined lanes with other barcoded projects (Table S2).
166 *Sequence alignments and SNP calling*
167 We combined our dataset of 33 samples with five previously published samples
168 (Stankowski et al., 2019) from the *Mimulus aurantiacus* species complex as an outgroup for
169 analysis. *M. aurantiacus* is outside of section *Eunanus* but is the closest group with previous
170 genome-scale data, as well as the closest group for which a reference genome assembly is
171 currently available. For all 38 samples, we trimmed raw sequencing reads using Trimmomatic
172 v0.39 (Bolger et al., 2014) to remove adapters and low-quality ends. We mapped reads to the
173 *Mimulus aurantiacus* reference genome (Stankowski et al., 2019) using bwa mem v0.7.17 (Li &
174 Durbin, 2009), then sorted and indexed with samtools v1.10 (Danecek et al., 2021). We

175 removed PCR duplicates using the MarkDuplicates tool in Picard v2.21.6 (Broad Institute, 2019),
176 and removed reads with unmapped mate pairs or mapping quality <29 using samtools view
177 (Danecek et al., 2021). Average read coverage per sample was 2.2-15.7 (mean 6.8) across 33
178 novel samples (details in Table S1).

179 We called SNPs in each sample using the GATK v4.1.6.0 haplotype caller, then used GATK
180 GenotypeGVCFs to jointly call variant and invariant sites for the entire dataset in 'all-sites'
181 mode (Van der Auwera & O'Connor, 2020). Only sites mapping to the ten major linkage groups
182 of the reference genome, corresponding to ten nuclear chromosomes, were included. We split
183 the resulting VCF into SNPs and invariant sites, and separately filtered each before recombining
184 them into a joint dataset, following recommendations by Dmitri Kryvokhyza (Kryvokhyzha,
185 2022). We filtered both SNPs and invariant sites to remove sites with combined DP <83 (~1/3 of
186 mean combined depth) or >1376 (two standard deviations above mean combined depth),
187 QD<2, SOR>3, or MQ<40. We additionally filtered SNPs to keep only biallelic sites across the
188 entire dataset, and to remove sites with QUAL<40, FS>60, MQRankSum<-12.5,
189 ReadPosRankSum>12.5, or ReadPosRankSum<-12.5.

190 Starting with all sites that pass the above filters (14,814,282 biallelic SNPs and
191 96,871,941 invariant sites), we generated four datasets for analysis. For genome-wide
192 phylogenetic and introgression analyses, we used a 'complete' dataset, which retained only
193 sites where fewer than 30 of 38 (approximately 80%) of samples had a called genotype,
194 resulting in 7,728,322 biallelic SNPs and 32,658,171 invariant sites. When calculating genome-
195 wide introgression metrics, we also attempted to reduce stemming from uneven sampling of
196 species and uneven coverage across individuals, by creating a 'downsampled' dataset of

197 equalized sampling and coverage. For this set, we chose the two most divergent individuals
198 from each species (except for *M. constrictus* for which we only had one sample), then randomly
199 sampled 12 million raw read pairs from each individual and used the same pipeline as above to
200 generate SNPs and invariant sites. Again, we retained only sites where 10 of 13 samples (~80%)
201 had called genotypes, resulting in 3,778,609 SNPs and 26,939,196 invariant sites.

202 For the calculation of diversity and divergence metrics, we made a 'synonymous sites'
203 dataset. Starting with the 'complete' dataset, we used the *M. aurantiacus* gene annotation to
204 select only sites in the 3rd codon position of coding sequences that were four-fold degenerate,
205 i.e., any nucleotide change to that site in the reference background would not change the
206 protein sequence, using a custom script by Tim Sackton (Sackton, 2014/2022). The
207 'synonymous sites' dataset included 967,470 SNPs and 1,654,798 invariant sites. We note that
208 multiple mutation hits within a single codon are possible given the large proportion of variant
209 sites across the dataset, which could change the synonymous nature of these sites, but we
210 expect these events to be rare enough to not substantially affect our genome-wide results on
211 average.

212 For gene-by-gene analyses, we used a 'genic' dataset that included all sites passing the
213 initial filters that fell within each of the 22,421 genes in the *M. aurantiacus* genome annotation.

214 *Phylogenetic tree building*

215 To determine phylogenetic relationships among our samples, we built a maximum
216 likelihood phylogenetic tree using the GTR+Gamma model in RAxML v8.2.12 (Stamatakis, 2014)
217 with SNPs from the 'complete' dataset. SNPs were extracted into a concatenated fasta
218 alignment using the 'consensus' function from bcftools v1.13 (Danecek et al., 2021) and

219 invariant sites were excluded. Heterozygous sites were initially coded as IUPAC ambiguity
220 codes, then randomly converted to a single allele with the 'randbase' function in seqtk v1.3 (Li,
221 2018). We ran 10 separate iterations of RAxML with unique random seeds, then chose the
222 iteration with the largest log-likelihood. We used the RAxML -b option to run 1000 rapid
223 bootstrap trees. We also generated a neighbor-joining tree with 1000 bootstrap replicates from
224 the same data, using the dist.ml, nj, and boostrap.phyDat functions in the R package phangorn
225 (Schliep, 2011).

226 We generated gene trees to examine patterns of gene tree discordance on the
227 phylogeny. We used SNPs from the 'genic' dataset in the *M. aurantiacus* genome annotation,
228 following the same approach as above to generate a maximum-likelihood phylogenetic tree in
229 RAxML for each gene. Genes with insufficient data to resolve a tree (any individual with no
230 called sites, or any two individuals with identical sequence) were excluded, resulting in trees for
231 17,573 genes. We then input these trees into ASTRAL v5.6.1 (Rabiee et al., 2019) which uses a
232 multispecies coalescent approach to calculate a consensus species tree and quartet support
233 scores for each node.

234

235 *Quantifying homozygosity, diversity, and divergence*

236 Pairwise sequence differences were calculated from the 'synonymous sites' dataset using
237 the 'dxy' and 'pi' functions in the program pixy v1.2.3 (Korunes & Samuk, 2021). For each
238 comparison, sequence differences were calculated in 1Mb windows across the genome, then
239 added together and divided by the total number of informative sites. We calculated pairwise
240 diversity (π_s) for each pair of individuals within a species, pairwise divergence (d_s) for each pair

241 of individuals across species, and heterozygosity (h_s, pairwise diversity within an individual) for
242 each individual. Diversity, divergence, and heterozygosity values were averaged across
243 individuals within each species, or across individual pairs within each species pair.
244 To estimate the divergence times between species, we used the following molecular
245 clock formula: (divergence time in generations) = (synonymous divergence – synonymous
246 ancestral diversity)/(2*mutation rate). We assumed ancestral diversity for any two species to
247 be the average of within-species diversity for the two species, and took the mutation rate to be
248 1.5x10^-8 (Koch et al., 2000). These estimates are approximate, as they do not take into
249 account the effect of changing effective population sizes, such as demographic bottlenecks, or
250 the possibility that ancestral diversity was very different from current diversity.
251
252 *Quantifying introgression*
253 To explore historical introgression between species, we used three complementary
254 approaches: ABBA-BABA tests and the related *f*-statistics; gene tree discordance bias using
255 TWISST; and the model-based TreeMix program.
256 We used Dsuite v0.4 (Malinsky et al., 2021) to calculate Patterson's D, a measure of the
257 relative frequency of ABBA and BABA sites in the genome, and the related *f4* statistic, which
258 uses allele frequencies to estimate the proportion of the genome resulting from introgression.
259 We calculated D and *f4* for all possible trios of species in our dataset, using both the 'complete'
260 and 'downsampled' SNP datasets, with the *M. aurantiacus* complex as the outgroup. Z-scores
261 and associated p-values were calculated for each trio using a block-jackknife approach with 100
262 blocks in Dsuite; to account for multiple tests, a Bonferroni correction was used to obtain a

263 corrected p-value (p_{corr}). Because there are multiple trios available to estimate introgression for
264 the same pair of species, we summarized results across trios using the F_{branch} statistic in Dsuite
265 for each species pair (Malinsky *et al.* 2018).

266 We used TWISST (github version d56cefb) (Martin & Van Belleghem, 2017) to obtain the
267 proportion of gene trees supporting particular tree topologies. For each trio of species, we
268 compared the two possible alternate (different from the consensus specie tree) tree topologies
269 using a binomial test with expected ratio 1:1 to look for an excess of one topology over
270 another. The *M. aurantiacus* complex was always used as the outgroup. This test is analogous
271 to the SNP-based ABBA-BABA test, but uses gene trees rather than SNPs.

272 We used TreeMix (Pickrell & Pritchard, 2012) to create phylogenetic network models
273 with or without migration edges as a further test of introgression. We used the 'synonymous
274 sites' dataset, including only variant SNPs with no missing data, and grouped individuals by
275 species. The dataset was pruned to select SNPs not in linkage disequilibrium using a custom
276 script by Joana Meier (https://github.com/joanam/scripts/raw/master/ldPruning.sh). We ran
277 models with zero to four migration edges, with 10 replicate runs per model type. The program
278 OptM (Fitak, 2021) was used to define the best fitting TreeMix migration model.

279

280 *Identifying candidate windows with historical introgression*

281 To identify candidate genomic regions with signatures of historical introgression, we
282 used Dsuite (Malinsky et al., 2021) to calculate the window-based *df* statistic (Pfeifer and
283 Kapan, 2019) for windows of 100 informative SNPs, each overlapping the previous by 50 SNPs.
284 We calculated *df* across the genome for three focal trios with strong support for introgression,

285 using the *M. aurantiacus* complex as the outgroup. In each quartet, we selected the 100
286 windows (out of 9594 to 17530, depending on the quartet) with the most extreme (positive or
287 negative) values as potential candidates of introgression, with positive values set to match the
288 direction of the genome-wide F_{branch} signal.
289
290 *Measuring reproductive barriers*
291 We assessed three different barriers to reproduction: postmating prezygotic isolation,
292 F1 hybrid seed inviability, and F1 hybrid sterility. We conducted hand pollinations of
293 greenhouse-grown plants within and among species by first removing anthers from the
294 maternal flower to prevent self-pollination, then using forceps to place pollen from the paternal
295 flower on the maternal stigma surface. Stigma lobes in these species close quickly in response
296 to touch, so hand-pollination is not always successful. In a few cases, supplemental pollen from
297 the same paternal plant was added the following day once the stigma had re-opened. We
298 collected mature, browned fruits, categorized according to cross type. Cross type throughout
299 this paper refers to the combination of maternal species and paternal species, with maternal
300 species always listed first; the 16 cross types are JxJ, JxB, BxJ, JxF, FxJ, JxS, SxJ, BxB, BxF, FxB,
301 BxS, SxB, FxF, FxS, SxF, SxS where J=*M. johnstonii*, B=*M. brevipes,* F=*M. fremontii*, S=Sespe creek
302 population. For the cross type BxF, we also germinated and grew F1 hybrids from four
303 independent crosses in the same conditions as parental plants (Table S3). These F1 hybrids
304 were crossed to themselves and reciprocally with *M. fremontii* and *M. brevipes* as above (cross
305 types HxB, BxH, HxH, HxF, FxH, where H=F1 hybrid). F1 hybrids between other species pairs
306 were not grown because of low crossing success or low seed viability.

307 To measure postmating prezygotic isolation, we quantified crossing success (probability
308 that a pollination produces at least one seed) and seed production (number of seeds per fruit)
309 after hand-pollination; both viable and inviable seeds were included but unfertilized ovules
310 were not. To test for an association between cross type and crossing success, we ran a
311 penalized Firth regression with a binomial family function using the R package 'brglm'. A Firth
312 regression was chosen to account for complete separation (all successes or all failures) of some
313 groups. To test the dominance relationships of this barrier, we compared the crossing success
314 of *M. brevipes* x *M. fremontii* F1 hybrids to their parental species. We ran a generalized linear
315 mixed-effects model (GLMM) with a binomial family and logit link function using the R package
316 'lme4' on cross types BxB, BxH, BxF, HxB, HxH, HxF, FxB, FxH, and FxF, where H indicates F1
317 hybrid offspring from a BxF cross. For this model, maternal population was included as a
318 random effect, treating each independent F1 cross as its own population.
319 To assess seed viability in each cross, we used a combination of visual inspection and
320 chemical treatment. All seeds were inspected under a dissecting scope and scored as inviable or
321 viable. Viable seeds were plump and generally ovate, although they were allowed to be slightly
322 misshapen as long as they appeared to be full. Inviable seeds included any seed that was
323 severely shriveled, concave, empty, much smaller than the typical within-species seed, or with a
324 shape very different from the typical ovate shape. To confirm that seeds visually scored as
325 inviable were in fact inviable, we treated a subset of seeds with tetrazolium chloride, which
326 stains viable seeds dark red. For this treatment, seeds were scarified using 1:5 bleach:distilled
327 water with 0.83 uL/mL Triton-X for 15 minutes, washed twice with distilled water, and placed in
328 1% (w/v) tetrazolium chloride, then incubated in the dark at room temperature for ~48 hours.

329 To test for an association between cross type and the relative counts of viable vs. inviable
330 seeds, we ran a penalized Firth regression using the R package 'brglm' with a binomial family
331 and logit link function. A Firth regression was chosen to account for complete separation (all
332 viable or all inviable) of some groups.

333 To investigate reciprocal differences in seed size, a predicted correlate of parental
334 conflict-driven hybrid seed inviability (Haig & Westoby, 1991), we imaged a subset of seeds
335 from 49 fruits under a dissecting scope and used imageJ to manually measure seed length and
336 width. This included all available seeds for those cross types with few seeds, and a random
337 selection of seeds from a random selection of fruits for other cross types. We ran a linear
338 mixed-effects model using the R package 'lme4' to test for differences in seed length between
339 the four intraspecific cross types (JxJ, BxB, FxF, and SxS), using fruit as a random effect. We also
340 ran six independent LMMs, one for each pair of species, to directly compare intra- and
341 interspecific seeds. For example, we tested the *M. johnstonii* vs. *M. brevipes* pair by comparing
342 cross types JxJ, JxB, BxJ, BxB. For each species-pair, we ran one LMM to test for an association
343 between cross type and seed length, and a second to test for an association between cross type
344 and seed length/width ratio.

345 To assess hybrid male sterility of *M. brevipes-M. fremontii* F1 plants compared with their
346 parental species, we scored pollen number and pollen viability using an aniline blue stain. For
347 each individual, all anthers from a single flower were collected in 50 µL 0.25% aniline blue in
348 lactophenol solution. Blue stained pollen grains were scored as viable, while unstained clear
349 pollen grains were counted as inviable. Pollen was counted in full $1mm^2$ squares of a
350 hemocytometer until 9 squares or at least 100 total pollen grains were counted. For each

individual, we estimated pollen viability by determining the proportion of viable pollen grains out of the total counted (for some individuals, pollen viability was measured from multiple flowers and the average was used). We used an LMM to test for an association between species ID and the total count of pollen grains scored per hemocytometer square, with population as a random effect. Similarly, we used a GLM with a binomial family and logit link function to test for an association between species ID (*M. brevipes, M. fremontii,* or F1 hybrid) and the relative counts of viable vs. inviable pollen grains, adding population as a random effect (each hybrid family was treated as its own population).

To assess *M. brevipes-M. fremontii* F1 female fertility, we hand-pollinated F1 hybrids with pollen from either parent and measured seed production. To determine whether F1 hybrids produce fewer seeds than within-species crosses, we used a linear model to test for an association between cross type and the number of seeds produced per fruit, comparing cross types BxB, BxH, HxF, and FxF and only counting fruits that produced at least one seed.

For every statistical model above, we ran Tukey post-hoc tests implemented in the package 'multcomp' to test for pairwise differences between each cross type or group.

We followed the methods of Sobel and Chen (2014) to calculate standardized measures of reproductive isolation for each of three reproductive barriers, as well as total postmating reproductive isolation, between each species. All measures used the equation

$$RI = 1 - 2 * (H/(H + C))$$

where H=heterospecific fitness and C=conspecific fitness. In this framework, RI ranges from -1 to 1 where -1 is complete heterosis, 0 is random assortment, and 1 is complete isolation. We calculated total measured reproductive isolation sequentially with the equation

373 $$RI_{TOTAL} = RI_{previous} + \left(1 - RI_{previous}\right) * RI_{new}$$

374 where $RI_{previous}$ is the total RI from all previous barriers and RI_{new} is the next barrier. Barriers that

375 could not be measured due to complete or near-complete previous RI were left blank.

376

377 **RESULTS**

378 **Genome-wide variation in the *M. brevipes* group defines clear species but also reveals a**

379 **complex history of introgression.**

380 A maximum-likelihood phylogeny generated from whole-genome SNP data resolves each

381 of the three focal species (*M. brevipes*, *M. johnstonii*, and *M. fremontii*) as monophyletic with

382 100% bootstrap support (Figure 1C). Within these species, each population is also recovered as

383 monophyletic, with the exception of one sample from a *M. brevipes* population (Figure 1C: one

384 individual from population B11 clusters with B19). *M. johnstonii* is supported as sister to *M.*

385 *brevipes,* in contrast to (Beardsley et al., 2004) which found *M. brevipes* and *M. fremontii* as

386 sister based on just three loci. Genome-wide estimates of pairwise nucleotide divergence at

387 synonymous sites also support strong divergence among the three focal species, with pairwise

388 divergence values (d_s, 4.8-6.0%) consistently well outside the range of nucleotide diversity

389 within species (π_s, range 1.6-3.7%) (Figure 1D, Table S4). Heterozygosity is similar to pairwise

390 diversity (h_s, range 1.1-3.1%), supporting a primarily outcrossing strategy in these species.

391 Speciation times were estimated at >1 million generations for all species pairs (Figure 1C).

392 The Sespe Creek population (S25) is clearly a distinct lineage well outside of the *M.*

393 *brevipes* trio. Although S25 is most closely related to *M. constrictus*, high genetic divergence

394 between these lineages (d_s = 0.06) suggest that S25 is a distinct species (Figure 1D, Table S4).

395 Other species in this clade are not sampled and could be closer relatives to Sespe Creek, but
396 none are known to occur in that geographic area. *M. nanus* is recovered as an outgroup to the
397 other *Eunanus* section species as expected, with the *M. aurantiacus* complex set as the ultimate
398 outgroup (Figure 1C). Species-level relationships from the maximum-likelihood tree were
399 corroborated by a neighbor-joining tree and ASTRAL consensus tree (Figure S1).

400 Despite clear divergence between these *Mimulus* species, we also discovered
401 substantial historical introgression. Using ABBA-BABA tests (Table 1, Table S5) and associated *F*
402 statistics (Figures 2A and S2), TWISST (Figure S3), and TreeMix (Figure S4), we detected three
403 signals of gene flow that were consistent across all methods. The first of these signals supports
404 directional introgression from the *M. brevipes-M. fremontii-M. johnstonii* clade into the Sespe
405 Creek population (Table 1: D = 0.135-0.149; Figure 2A: F_{branch} = 4.8-5.9%, Figure S3: TWISST
406 quartets 41.1/41.8/17.0, Figure S4: TreeMix m=0.193). A second, weaker signal of introgression
407 occurs in the reciprocal direction from the *M. constrictus*-Sespe Creek clade into the *M.*
408 *brevipes-M. fremontii-M. johnstonii* clade (Table 1: D = 0.027-0.046, Figure 2A: F_{branch} = 0.4-
409 1.3%, Figure S3: TWISST quartets 70.3/15.7/14.0, Figure S4: TreeMix m=0.021). Finally, a third
410 signal of introgression was detected between *M. nanus* and the clade containing *M. constrictus*
411 and Sespe Creek (Table 1: D = 0.101-0.178, Figure 2A: F_{branch} = 2.4-3.4%, Figure S3: TWISST
412 quartets 73.5/15.2/11.3, Figure S4: TreeMix m=0.296). We summarize these patterns in Figure
413 S5, but note that shared evolutionary history makes it challenging to assign introgression events
414 to single lineages.

415 For each of these three general cases, we chose the trio with the strongest signal and
416 scanned the genome for signatures of introgression using the statistic *df*. Outlier *df* windows

417 were asymmetric, with more positive outliers (signals of introgression consistent with the
418 genome-wide F_{branch} pattern) than negative outliers of the same magnitude (Figure 2B). Positive
419 outliers were widely distributed throughout the genome, present on all ten linkage groups for
420 all three trios and with no large blocks of uninterrupted introgression, indicating that gene flow
421 in this group is ancient rather than ongoing.
422
423 **Multiple strong postmating reproductive barriers between species in the *M. brevipes* group.**
424 Most crosses between four focal species (*M. johnstonii, M. brevipes, M. fremontii,* and
425 the Sespe Creek population) showed little to no reduction in crossing success (probability of
426 producing a seed, or seeds produced per fruit) compared to within-species crosses (Figures 3
427 and S6, Table S6). In one case (FxB), there is evidence of strong unidirectional postmating
428 prezygotic isolation: only one in 58 crosses between maternal *M. fremontii* and paternal *M.*
429 *brevipes* produced any seeds, a significantly lower proportion than the within-species or
430 reciprocal cross types (Figure 3, Table S6). This pattern appears to be additive on both the
431 maternal and paternal sides in *M. brevipes* x *M. fremontii* F1 hybrids, with intermediate crossing
432 success in both HxB and FxH crosses (Figure S7). A few other interspecific cross types also had
433 low or zero seed production (e.g., reciprocal crosses of *M. fremontii* and Sespe Creek), which
434 could indicate a postmating prezygotic barrier, but these crosses had low sample sizes and did
435 not reach significance compared to within-species crosses.
436 For crosses that did produce seeds, we found strong F1 hybrid seed inviability (viability
437 <2%) in nine interspecific crosses (Figure 4A-B, Table S6). The exception was species pair *M.*
438 *fremontii* and *M. brevipes,* which produced viable seeds in both directions (Figure 4A-B, Table

439 S6). We could not score seed viability for cross type SxF because the only potential seeds
440 produced were not distinguishable from unfertilized ovules.

441 *M. johnstonii* intraspecific seeds were significantly larger than *M. brevipes* or *M.*
442 *fremontii* seeds, with Sespe Creek seeds intermediate in size (Figure 4C, Table S7). Inviable
443 seeds overall showed no evidence of overgrowth or undergrowth relative to parents, but
444 instead tended to match the seed length of the maternal parent. However, F1 hybrids with
445 Sespe Creek as maternal parent did have slightly smaller seeds than either parent (this trend
446 was only significant for SxF) (Figures 4A and S8A, Table S7). Crosses with *M. johnstonii*, the
447 largest-seeded species, as the maternal parent produced inviable seeds that were collapsed and
448 thin, as shown by a significant increase in hybrid seed length/width ratios (three cross types)
449 compared to both parents and to the reciprocal cross type (Figures 4A and S8B, Table S7). In the
450 reciprocal direction, hybrid seeds were typically shriveled, as were hybrid seeds in both
451 directions of Sespe Creek crosses (Figures 4A and S8B).

452 Although in most cases, strong seed inviability prevented us from quantifying later-
453 acting barriers, we were able to assess F1 hybrid sterility between *M. brevipes* and *M.*
454 *fremontii*. Pollen number per flower was intermediate for hybrids compared to the two
455 parental species (Figure 5A, Table S8). However, only ~20% of hybrid pollen grains were fertile,
456 a sharp reduction from either parent, indicating strong F1 male sterility (Figure 5B, Table S8).
457 We find no evidence of hybrid female sterility in *M. brevipes* x *M. fremontii* F1s; seed
458 production from pollinated hybrids was intermediate compared to pure species (Figure 5C).

459 Total postmating reproductive isolation was near-complete (RI>=0.95) for all tested
460 species pairs except for *M. brevipes* vs. *M. fremontii,* primarily driven by strong hybrid seed

461 inviability (Table 2). The exception, *M. brevipes* vs. *M. fremontii,* had incomplete but still
462 substantial total postmating RI from a combination of postmating prezygotic isolation and F1
463 male sterility (B > F: RI=0.91; F > B: RI=0.66).
464

465 **DISCUSSION**

466 A major goal of speciation research is to understand similarities and differences in how
467 reproductive isolation emerges as groups of species diverge. We find that *Mimulus brevipes,*
468 *Mimulus johnstonii, and Mimulus fremontii* are clearly delineated species both genetically and
469 by intrinsic reproductive barriers. We find strong hybrid seed inviability between multiple
470 species pairs, as well as a postmating prezygotic barrier and severe hybrid male sterility
471 between one species pair. While premating barriers have not yet been thoroughly quantified in
472 this group, the combination of close geographic proximity (within centimeters in some cases)
473 and similar floral morphology (excluding *M. brevipes*) makes it unlikely that premating barriers
474 alone can eliminate hybridization. These strong postmating barriers are therefore likely to be
475 important in preventing contemporary gene flow.

476 While many studies have shown that reproductive isolation increases with divergence
477 on average, individual species pairs are often idiosyncratic (Coyne & Orr, 1989; Malone &
478 Fontenot, 2008; Matute & Cooper, 2021; Moyle et al., 2004). Our results highlight this
479 heterogeneity – while reproductive isolation and divergence are both strong overall, the
480 species pair with the least postmating reproductive isolation in this group (*M. brevipes* and *M.*
481 *fremontii*) is not the most recently diverged pair (*M. brevipes* and *M. johnstonii*). Paying greater

482 attention to the exceptions may help us better understand the factors that drive reproductive
483 isolation.

484 *Gene discordance and introgression*

485 We find evidence of extensive phylogenetic discordance across the genome, including
486 signatures of historical introgression between multiple species in this group. These signals are
487 scattered throughout the genome and broken up by generations of recombination; we find no
488 evidence of recent or ongoing introgression. Without further sampling of populations and
489 species in this section, attributing these signals to precise events on the phylogeny is difficult.
490 Taken as a whole, however, they demonstrate a high degree of complexity in the divergence
491 process, consistent with reticulate evolutionary histories of other groups within *Mimulus* (e.g.,
492 Brandvain et al., 2014; Nelson et al., 2021; Stankowski et al., 2019), in plants more broadly (e.g.,
493 Curtu et al., 2009; Goulet et al., 2017; Hamlin et al., 2020; Kay et al., 2018; Scascitelli et al.,
494 2010), and across the tree of life (e.g., D'Angiolo et al., 2020; Green et al., 2010; Kleindorfer et
495 al., 2014; Mallet et al., 2007; Schumer et al., 2018). Without postmating reproductive barriers,
496 even small amounts of introgression can lead to species collapse in sympatry, especially if
497 premating barriers are disrupted by environmental change (Behm et al., 2010; Kleindorfer et
498 al., 2014; Xiong & Mallet, 2022). Alternatively, species can persist despite ongoing
499 introgression, depending on the circumstances (Kay et al., 2018; Kenney & Sweigart, 2016;
500 Servedio & Hermisson, 2020). Past introgression in the *Eunanus* group may have predated the
501 evolution of the strong postmating barriers we see today. We argue that postmating
502 reproductive barriers likely played an important role in reducing gene flow as divergence

503 increased, contradicting the hypothesis that postmating barriers are 'after-the-fact' byproducts
504 with little influence on speciation trajectories.

505 *Cryptic diversity in Mimulus section Eunanus*

506 Genetic data allow us to uncover cryptic variation in the form of distinct genetic lineages
507 that are not readily distinguished by morphological features in the field (Bickford et al., 2007;
508 Struck et al., 2018). Our population from Sespe Creek does not appear to match any of the
509 likely species from the area, and we find that it is a genetically distinct lineage with a history of
510 introgression. In addition, it appears to be reproductively isolated from other members of the
511 group by strong hybrid seed inviability. We do not yet know the exact nature of its origin, or
512 how widely distributed this lineage is; more sampling from the area and genetic data from
513 more species in the group will be necessary to fully resolve these questions. Studies of
514 speciation in plants often focus on ecologically mediated premating reproductive isolation, but
515 cryptic diversity may be better explained by postmating barriers (Coughlan & Matute, 2020).
516 *Mimulus* section *Eunanus* is home to many more understudied, small, pink-flowered taxa; if our
517 study is any indication, strong postmating reproductive isolation may play an outsized role in
518 generating diversity in this group.

519 *Parallel evolution of hybrid seed inviability in Mimulus*

520 Hybrid seed inviability has been found repeatedly in species pairs from the *Mimulus*
521 *guttatus* species complex (section *Simiolus*) (Coughlan et al., 2020; Oneal et al., 2016; Sandstedt
522 & Sweigart, 2022). By demonstrating hybrid seed inviability in a distant section of *Mimulus,* we
523 show that this pattern is widespread and important, both across *Mimulus* and likely in plants
524 more broadly. In the *M. guttatus* complex and other systems, hybrid seed inviability has been

525 tied to parental conflict in resource allocation, a process mediated by the endosperm (Coughlan
526 et al., 2020; Haig & Westoby, 1991; Lafon-Placette et al., 2017; Oneal et al., 2016; Rebernig et
527 al., 2015; Roth et al., 2019; Sandstedt & Sweigart, 2022). We do not find clear evidence of
528 parental conflict in our system -- hybrid seed sizes tended to track maternal seed sizes, without
529 the telltale overgrowth or undergrowth phenotypes. However, hybrid seed size is not always a
530 good predictor of parental conflict (Sandstedt & Sweigart, 2022), so future work to characterize
531 differences in seed development would be required to rule out a conflict hypothesis.
532 Alternatively, differences in parental seed sizes between our species could result in
533 Dobhzansky-Muller-like incompatibilities during hybrid seed development, without invoking
534 parental conflict as a driver. Seed size is an important life history trait tied to ecological
535 strategies; larger seeds tend to have more success establishing under a variety of hazardous
536 conditions, from nutrient deprivation to low soil moisture to deep burial (Leishman et al.,
537 2000). Larger, heavier seeds may also prevent long-range dispersal and keep offspring in
538 maternal habitats for which they are locally adapted, as is the case in dune-adapted plants
539 (Bowers, 1982; Schwarzbach et al., 2001). Both *M. johnstonii* and the Sespe Creek population
540 are found on unstable scree slopes, which may pose a particular challenge to seed
541 establishment or favor local dispersal to maintain local adaptation. This habitat preference is
542 therefore a possible candidate for a selective force, which could have acted in parallel in *M.*
543 *johnstonii* and Sespe Creek to drive seed size differences leading to hybrid inviability.
544 *Postmating prezygotic isolation*
545 Crossing failure (postmating prezygotic isolation) can be caused by a failure of pollen
546 tube germination, failure of pollen tube growth, failure of fertilization, or even early seed

547 abortion (Wheeler et al., 2001); it may be a passive incompatibility between pollen and pistil, or
548 an active rejection mechanism to prevent maladaptive hybridization (Hogenboom et al., 1975;
549 Roda & Hopkins, 2019; Rushworth et al., 2022). Most studies on the mechanisms of postmating
550 prezygotic isolation come from systems with self-incompatibility, where they are thought to be
551 related to self-incompatibility mechanisms, e.g. *Solanum* (Bernacchi & Tanksley, 1997; Tovar-
552 Méndez et al., 2014), *Nicotiana* (Kuboyama et al., 1994), and *Lilium* (Ascher & Drewlow, 1975),
553 though a mechanism unrelated to self-incompatibility has been described in *Brassica* (Fujii et
554 al., 2019). Since *Mimulus* lacks self-incompatibility mechanisms, this group provides an
555 opportunity to investigate how interspecific incompatibility may arise on its own. In other
556 systems with differences in style length, germinating pollen tubes can under- or over-shoot the
557 ovules (Gore et al., 1990; Williams & Rouse, 1988). Style length could be important in our
558 system, since *M. brevipes* styles are substantially longer than *M. fremontii* styles, though our
559 case is unusual in that pollen from the long-styled parent fails while pollen from the short-
560 styled parent is successful. Pollen competition driving differential coevolution of the pollen and
561 pistil is another possible source of incompatibilities (Brandvain & Haig, 2005; Skogsmyr &
562 Lankinen, 2002), a scenario which has been documented in the *M. guttatus* complex (Aagaard
563 et al., 2013; Fishman et al., 2008) and *Arabidopsis* (Takeuchi & Higashiyama, 2012).

564 *Hybrid male sterility*

565 Hybrid male sterility has been characterized multiple times in *Mimulus* sections Simiolus
566 and Erythranthe, with a variety of genetic causes, including a nuclear DMI interaction (Sweigart
567 et al., 2006), a cytoplasmic-nuclear interaction (Fishman & Willis, 2006), or underdominant
568 chromosomal rearrangements (Stathos & Fishman, 2014), but the relative frequency of these

569 mechanisms across plants is unknown. *M. brevipes* and *M. fremontii* are more genetically
570 divergent than most pairs for which male sterility has been studied, in *Mimulus* or elsewhere.
571 Since they still produce viable hybrids and sterility is not 100% complete, genetic mapping could
572 be used in the future to determine the mechanisms underlying sterility in this system, and the
573 degree of parallelism with other cases in *Mimulus.*

574 *Future directions*

575 As the first in-depth genomic and phenotypic investigation of speciation within *Mimulus*
576 section *Eunanus,* this study fills an important phylogenetic gap within the speciation literature,
577 helping to position the genus *Mimulus* as a leading model for broad phylogenetically informed
578 comparisons of how species form and diverge. Our study system highlights both universal and
579 idiosyncratic patterns in the speciation process; we add to a growing body of evidence that
580 hybrid seed inviability and hybrid male sterility are important barriers to gene flow in *Mimulus*
581 and across plant taxa; and we demonstrate the complexity of gene discordance and historical
582 introgression among species despite substantial overall divergence. In addition, we lay the
583 groundwork for fruitful avenues of future mechanistic study: seed size evolution and hybrid
584 seed inviability; style length and postmating prezygotic isolation; and highly divergent hybrid
585 male sterility are all worthy of future exploration in this group. Out study also provides the
586 starting point for a more complete phylogenetic sampling of section *Eunanus*, which would
587 enhance our understanding of cryptic divergence and the interplay between ecological,
588 geographic, and genetic forces driving the diversification of species.

589 **Author contributions**

590 Research conceived and designed jointly by M.C.F and A.L.S. Data collected and analyzed by
591 M.C.F. Manuscript written by M.C.F and A.L.S.

592 **Data accessibility**

593 All newly generated whole genome sequence data are deposited at the NCBI Sequence Read
594 Archive (accession PRJNA922914). Other data will be made available on Dryad Digital
595 Repository upon publication.

596 **Acknowledgments**

597 We thank James Sobel for seed collections, for advice on germination and growth conditions,
598 and for helpful discussions. Samuel Mantel, Makenzie Whitener, Natalie Gonzalez, and Emma
599 Chandler provided comments that improved the manuscript. Kelly Dyer, Jill Anderson, Casey
600 Bergman, Molly Schumer, John Willis, Jenn Coughlan, Elen Oneal, and Robert Franks also
601 contributed to useful discussions. This work is supported by the National Science Foundation
602 DEB1856180; the National Institutes of Health Predoctoral Training Grant 5T32GM007103, the
603 Society for the Study of Evolution Lewontin Award, and a UGA Plant Center Doctoral
604 Dissertation Improvement Grant.
605 The authors declare no competing interests.

606

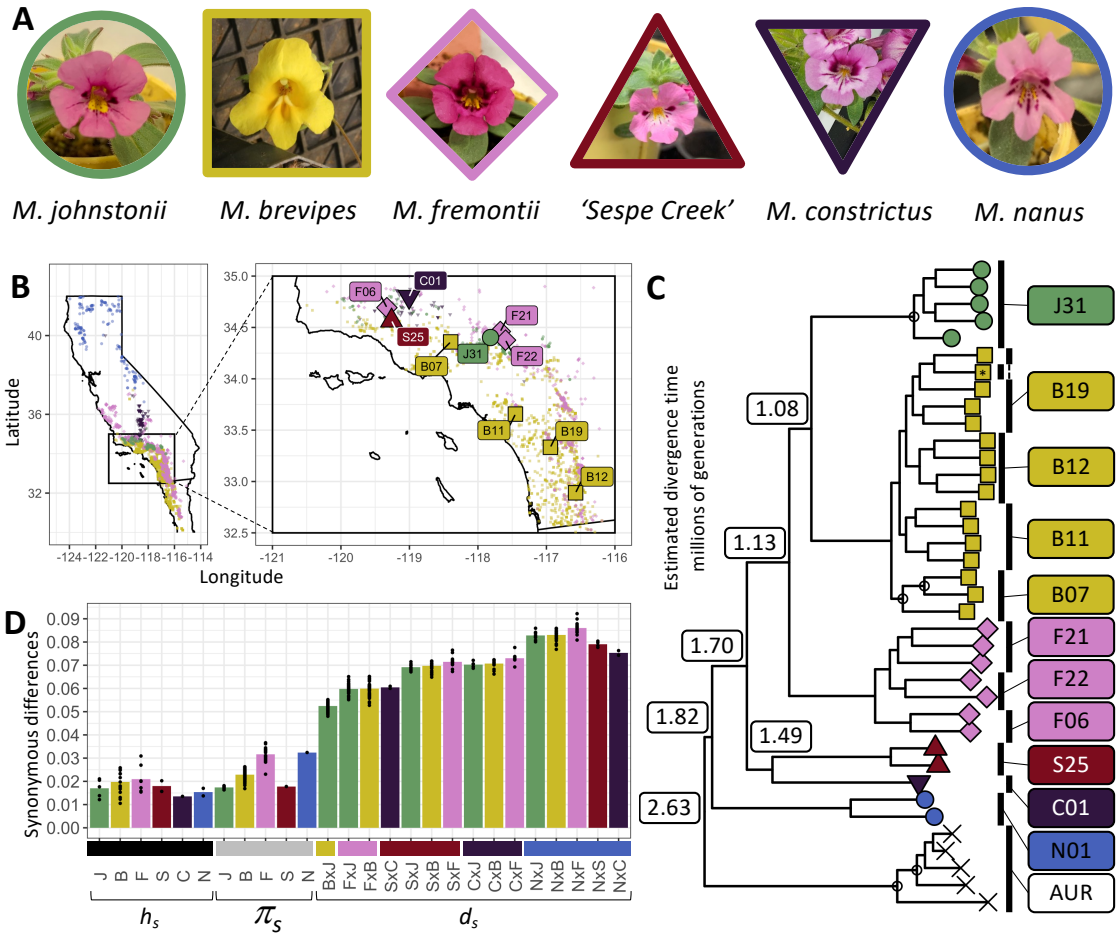

Figure 1. Phylogenetic relationships and divergence between sampled species in *Mimulus* section *Eunanus*. (A) Representative floral images for sampled species. (B) Map of occurrence records and sampled populations from the GBIF database for five species within California and Baja California. Inset highlights focal region for sampling, where species ranges overlap. Smaller icons indicate GBIF records (GBIF.org, 2022) for each species, which include iNaturalist research grade observations and herbarium collections. Larger named icons indicate sampled populations used in this study. The range of *M. nanus* extends into Nevada, Oregon, and Washington; population N01 (*M. nanus*) was collected from Washington state and is not shown. Population S25, referred to as Sespe Creek, is treated as a separate lineage. (C) Maximum likelihood phylogeny inferred using RAxML from the 'complete' dataset of genome-wide SNPs, rooted by the *M. aurantiacus* complex. All nodes except those marked with open circles have 100% bootstrap support. Species divergence times were estimated using synonymous divergence relative to synonymous diversity. All sampled populations are monophyletic with strong support, with the exception of one sample from B11 that clusters with B19 (marked with an asterisk). (D) Nucleotide heterozygosity (h_s), pairwise diversity (π_s), and divergence (d_s) at genome-wide synonymous sites, indicating substantially higher between-species divergence than within-species diversity. Bars represent species or comparison means, while points represent individual pairwise sample comparisons. Diversity includes both within- and between-population comparison where possible. Sespe creek is substantially diverged from

its closest sampled relative, *M. constrictus* (SxC d_s=6.0%). J = *M. johnstonii*, B = *M. brevipes,* F = *M. fremontii*, S = Sespe creek population, C = *M. constrictus*, N = *M. nanus*, AUR = *M. aurantiacus* complex.

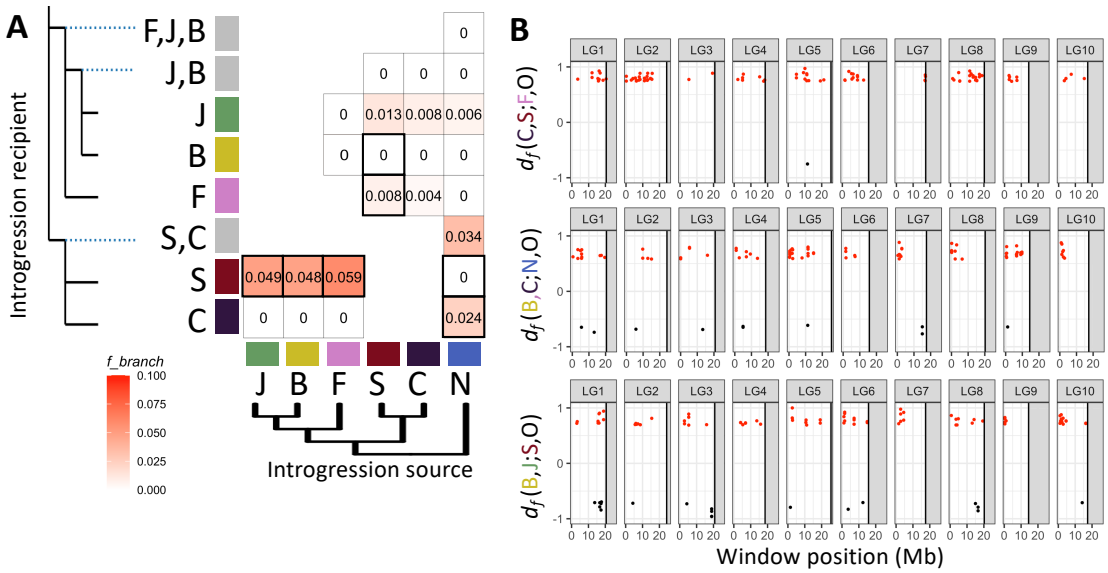

Figure 2. Signatures of historical introgression between species in *Mimulus* section *Eunanus*. (A) Genome-wide F_{branch} statistics, an estimate of the proportion of the genome affected by introgression based on correlated *f4* statistics, using the downsampled SNP dataset. All listed nonzero F_{branch} values are supported by ABBA-BABA tests with Bonferroni-corrected p-value < 0.001. Seven bold-outlined boxes indicate comparisons with significant gene discordance bias supporting introgression from TWISST gene tree summaries, using Bonferroni-corrected p-values <0.01. Full TWISST summaries are in Figure S3. (B) Position along ten linkage groups of extreme *df* values in 100-SNP windows for each of three tested quartets. Each quartet (P1,P2;P3,O) tests for signatures of introgression from P3 into P2 (positive outliers) or P3 into P1 (negative outliers). The top 100 windows with the largest absolute value of *df* are plotted, with positive *df* values in red and negative in black. From top to bottom, positive outliers show a history of introgression from *M. fremontii* into Sespe Creek, from *M. nanus* into *M. constrictus,* and from Sespe Creek into *M. johnstonii*. Total tested windows for each quartet: 9594, 10429, and 14596, respectively.

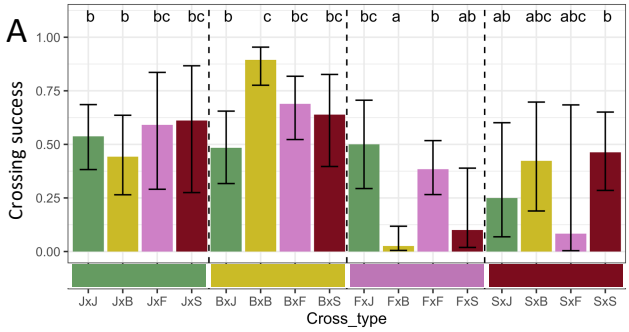

Figure 3. Postmating prezygotic isolation between at least one species pair. Crossing success (probability of producing at least one seed from a cross) for intra- and interspecific cross types. Shown are least-square means and asymptotic confidence intervals from a Firth binomial model. Letters indicate significance in post-hoc Tukey tests; cross types sharing a letter are not significantly different. One interspecific cross type, FxB, was significantly reduced compared to both intraspecific parental crosses, indicating an asymmetric barrier to fruit set. Two other crosses, FxS and SxF, had low fruit set possibly indicating a reproductive barrier, but were not significant in the model due to low sample sizes; e.g., 0 out of 4 SxF crosses resulted in seeds. J = *M. johnstonii*, B = *M. brevipes,* F = *M. fremontii*, S = Sespe creek population.

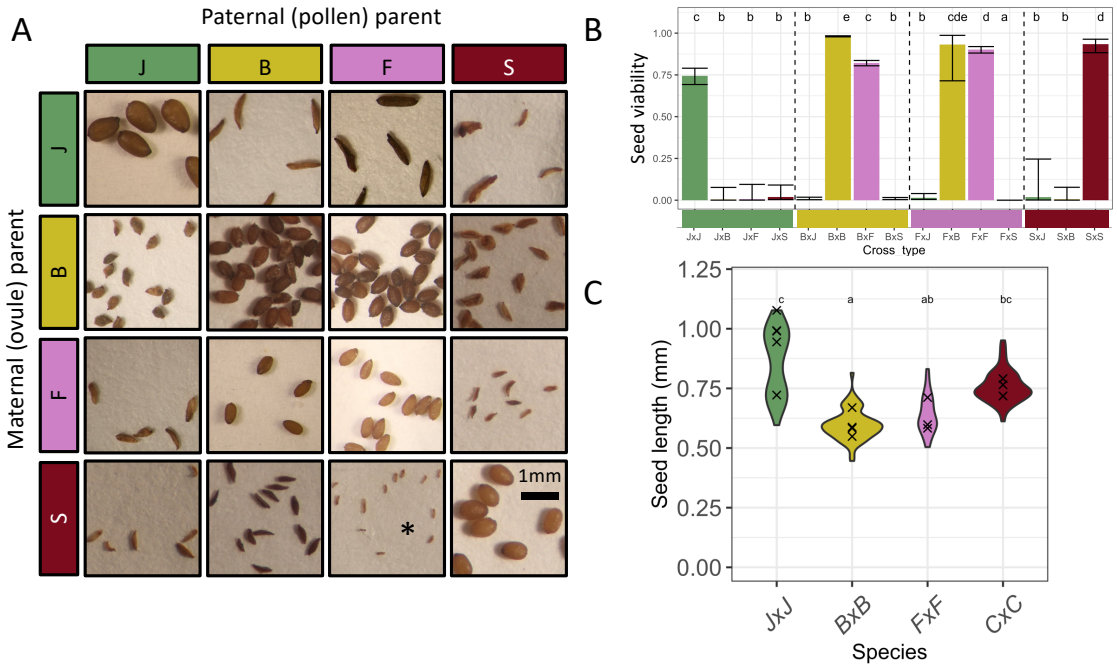

Figure 4. Strong hybrid seed inviability between multiple species pairs. (A) Representative seed images from intra- and interspecific laboratory crosses between four species. All images are adjusted to the same scale. For the SxF cross, marked with an asterisk, the only 'seeds' produced were not distinguishable from unfertilized ovules and were not counted as seeds for

663 crossing success or viability scoring, but it is possible they represent early seed abortion. (B)
664 Proportion of viable seeds produced by intra- and interspecific laboratory crosses. Shown are
665 least-square means and asymptotic confidence intervals from a Firth binomial model, with
666 letters indicating significance in post-hoc Tukey tests. Intraspecific, BxF, and FxB crosses are
667 mostly viable, but all other interspecific cross types have almost complete inviability. (C) Seed
668 lengths for intraspecific crosses. Violin plots show distribution of data for individual seeds, with
669 x's marking the means of individual fruits. Letters indicate significance from post-hoc Tukey
670 tests of an LMM.
671

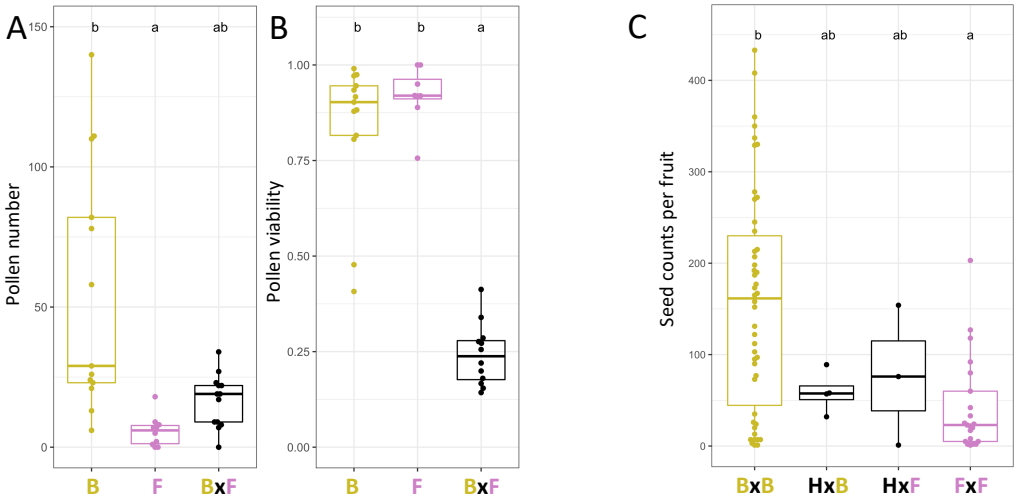

672
673 **Figure 5. Strong hybrid male sterility in hybrids between *M. brevipes* and *M. fremontii*.** (A)
674 Pollen number (counts per mm^2 on a hemocytometer) and (B) pollen viability (proportion of
675 pollen grains scored as viable in aniline blue stain). Letters indicate significance in post-hoc
676 Tukey tests from a poisson (abundance) or binomial (viability) GLMM with population as a
677 random variable. Each point represents the average across 1-3 flowers from a single individual.
678 For each panel, groups sharing a letter are not significantly different. (C) Seed production from
679 hybrid vs. parental fruits as a test of hybrid female sterility, including only fruits that produced
680 at least one seed. Letters indicate significance in post-hoc Tukey tests from a linear model.
681 B=*M. brevipes*, F=*M. fremontii*, H=*M. brevipes x M. fremontii* F1 hybrid.
682
683 **Table 1. ABBA-BABA test results from downsampled SNP dataset**.
684

P1	P2	P3	D	Z-score	Significance	*f4*-ratio	BBAA	ABBA	BABA
J	B	F	0.017	2.8	n.s.	0.009	97294	66664	64434
B	**J**	**S**	0.045	8.0	***	0.013	155429	53359	48765
J	F	S	0.007	1.4	n.s.	0.002	126129	59205	58393
B	**F**	**S**	0.047	9.4	***	0.015	129882	60335	54948
B	**J**	**C**	0.035	6.9	***	0.008	159203	46322	43188

F	J	C	0.005	0.9	n.s.	0.001	131898	51052	50586
B	**F**	**C**	0.027	5.7	***	0.007	135187	51425	48736
C	**S**	**J**	0.142	27.5	***	0.049	103893	69306	52109
C	**S**	**F**	0.149	27.2	***	0.059	103887	70221	52046
C	**S**	**B**	0.135	24.9	***	0.048	106972	68191	52012
B	**J**	**N**	0.031	7.6	***	0.006	215279	41581	39069
F	**J**	**N**	0.030	8.1	***	0.007	185137	46328	43605
F	B	N	0.003	0.8	n.s.	0.001	188742	44743	44481
J	**S**	**N**	0.102	24.3	***	0.028	124410	63335	51623
B	**S**	**N**	0.121	27.3	***	0.034	122382	65553	51390
F	**S**	**N**	0.124	31.0	***	0.034	126189	65090	50688
J	**C**	**N**	0.160	30.7	***	0.049	98813	68692	49743
B	**C**	**N**	0.176	31.9	***	0.055	97995	70669	49509
F	**C**	**N**	0.178	33.7	***	0.055	99391	70192	48945
S	**C**	**N**	0.087	16.9	***	0.024	136174	55129	46312

***p_{corr}<0.001. n.s.=not significant
J = *M. johnstonii*, B = *M. brevipes,* F = *M. fremontii*, S = Sespe creek population,
C = *M. constrictus*, N = *M. nanus*

Table 2. Summary of Postmating Reproductive Isolation (RI).

Pair a, b	Crossing success RI		Seed viability RI		F1 viability RI		**Total measured RI**	
	a>b	b>a	a>b	b>a	a>b	b>a	a>b	b>a
J, B	0.30	0.10	**0.99**	**1.00**	--	--	**0.99**	**1.00**
J, F	-0.13	-0.05	**0.97**	**1.00**	--	--	**0.97**	**1.00**
B, F	**0.91**	0.13	-0.03	0.09	--	**0.57**	**0.91**	**0.66**
J, S	0.35	-0.07	**1.00**	**0.97**	--	--	**1.00**	**0.96**
B, S	0.05	0.16	**1.00**	**0.99**	--	--	**1.00**	**0.99**
F, S	1.00	0.68	--	**1.00**	--	--	1.00	**1.00**

a>b indicates reproductive isolation preventing gene flow from species a into species b, calculated by comparing the fitness of b x a crosses relative to b x b crosses, with b>a indicating the reciprocal direction using the fitness of a x b crosses relative to a x a crosses, following (Sobel & Chen, 2014). **Bolded** values include contributions from barriers with significant model results.

Supplementary Figures and Tables

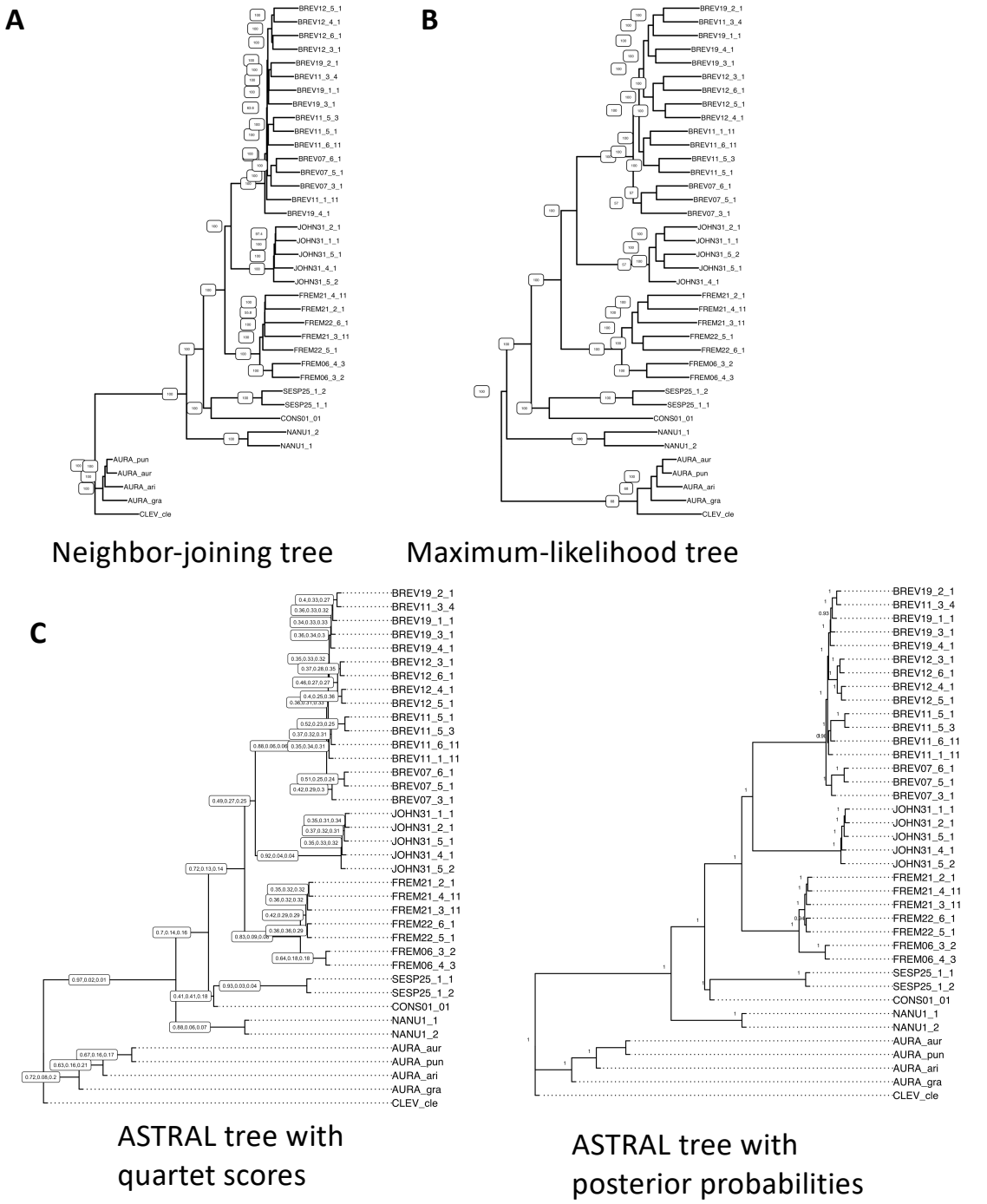

692
693 **Figure S1. Comparison of phylogenetic methods.** (A) Neighbor-joining tree produced from
694 'complete' SNP dataset, with heterozygous sites randomly assigned to one allele. (B) Maximum-
695 likelihood tree produced using RAxML from the 'complete' SNP dataset using the GTR+Gamma
696 model, with heterozygous sites randomly assigned to one allele. (C) ASTRAL tree produced from
697 17,524 gene trees, each created using RAxML with the GTR+Gamma model using SNPs from the
698 'genic' SNP dataset within a given gene's coordinates, with heterozygous sites randomly

assigned to one allele. Each node is labelled with the quartet support scores for the consensus, 1st alternative, and 2nd alternative topologies. (D) The same ASTRAL consensus tree shown in (C) but with posterior probabilities for each node.

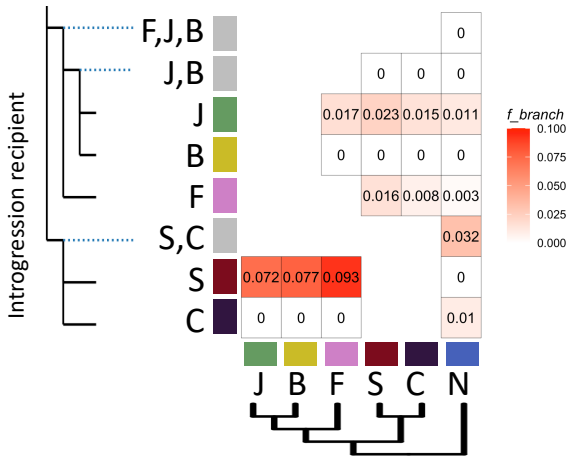

Figure S2. F_{branch} results 'complete' SNP dataset. Results are qualitatively consistent with the 'downsampled' dataset (Fig 2) but estimated F_{branch} values tend to be higher for the full dataset. J = *M. johnstonii*, B = *M. brevipes,* F = *M. fremontii*, S = Sespe creek population, C = *M. constrictus*, N = *M. nanus.*

Consensus topology	Alternate topology 1	Alternate topology 2	Binomial Test p_{corr}
C S F O 7207 (41.1%)	F S C O 7330 (41.8%)	F C S O 2987 (17.0%)	<0.001
C S J O 7,253 (41.4%)	J S C O 7,299 (41.6%)	J C S O 2,972 (17.0%)	<0.001
C S B O 7,183 (41.4%)	B S C O 7,287 (41.6%)	B C S O 3,054 (17.0%)	<0.001
F S N O 12,874 (73.5%)	N S F O 2,667 (15.2%)	N F S O 1,983 (11.3%)	<0.001
J S N O 12,869 (73.4%)	N S J O 2,613 (14.9%)	N J S O 2,042 (11.7%)	<0.001
B S N O 12,828 (73.2%)	N S B O 2,638 (15.1%)	N B S O 2,059 (11.7%)	<0.001
C S N O 12,312 (70.3%)	N S C O 2,773 (15.8%)	N C S O 2,439 (13.9%)	<0.001
F C N O 11,114 (63.4%)	N C F O 3,350 (19.1%)	N F C O 3,061 (17.5%)	0.006
B F S O 12,328 (70.3%)	S F B O 2,744 (15.7%)	S B F O 2,452 (14.0%)	0.001
J B F O 8,528 (48.7%)	F B J O 4,673 (26.7%)	F J B O 4,323 (24.7%)	0.004

Figure S3. TWISST gene tree discordance summaries. Twenty trios were tested, using *M. aurantiacus* as the outgroup in all tests. Shown are the ten trios with significant

overrepresentation of one alternate topology over another (binomial test, expected ratio 1:1, Bonferroni-corrected p_{corr}<0.05). For each trio, the number of genes support each topology are given, along with the percentage of total trees. A total of 17,524 genes were used for all trios. J = *M. johnstonii*, B = *M. brevipes,* F = *M. fremontii*, S = Sespe creek population, C = *M. constrictus*, N = *M. nanus*, O = *M. aurantiacus* complex.

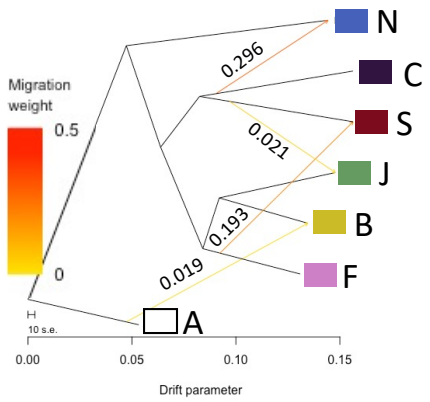

Figure S4. TreeMix network analysis results for four migration edges. The edge (C to N) was selected in the network with a single edge, which was the best model according to OptM; other edges improved the log-likelihood of the model by progressively decreasing amounts. Migration weights for the four-edge model are provided next to each edge.

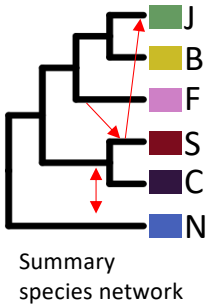

Figure S5. Summary of best-supported introgression events from multiple methods. Three introgression events were supported by f_{branch} , TWISST, and TreeMix results. The exact identity and direction of individual introgression events may be different due to shared ancestry and incomplete sampling; for example, signatures of introgression from all of *M. fremontii, M. johnstonii, and M. brevipes* into Sespe Creek may be caused by a single event in a common ancestor, an unsampled relative, or just one of the sampled species.

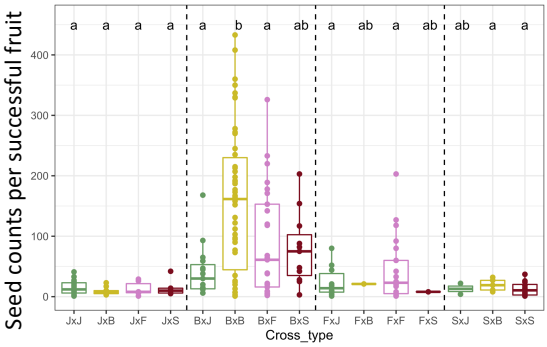

Figure S6. Seed counts do not indicate hybrid deficiency. Seed counts per fruit for fruits producing at least one seed. *M. brevipes* produces more seeds per fruit than the other species, but interspecific crosses do not show a reduction in seed count relative to intraspecific crosses. Letters indicate significance in post-hoc Tukey tests from a linear model; cross types sharing a letter are not significantly different.

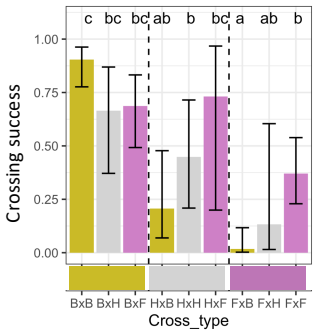

Figure S7. Crossing success in BxF hybrids is additive on maternal and paternal sides. Crossing success (probability of at least one seed produced from a cross) from crosses involving *M. brevipes* x *M. fremontii* F1 hybrids and their parental species. Shown are least-square means and asymptotic confidence intervals from a binomial GLMM. Letters indicate significance in post-hoc Tukey tests; cross types sharing a letter are not significantly different. HxB crosses have intermediate crossing success compared to BxB and FxB crosses (gold bars), indicating an additive effect of maternal species. Similarly, FxH crosses have intermediate crossing success compared to FxB and FxF crosses (right three bars), indicating an additive effect of paternal species. HxH have intermediate success compared to BxH and FxH (gray bars), as well as compared to HxB and HxF (middle three bars), further supporting additive patterns. B = *M. brevipes,* F = *M. fremontii*, H = F1 hybrids between *M. brevipes* and *M. fremontii*.

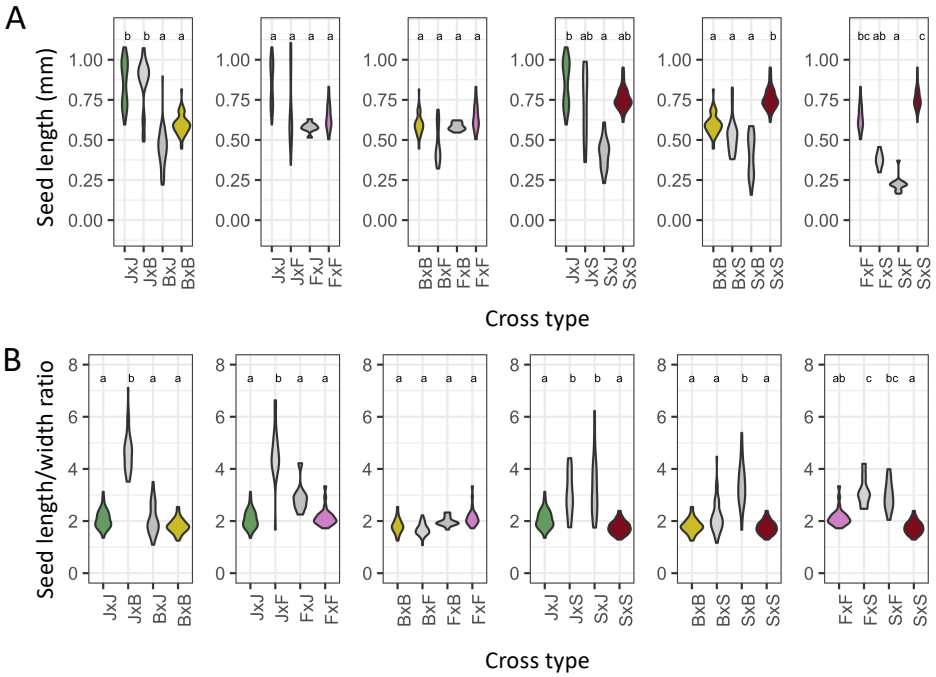

Figure S8. Seed measurements for all intra- and interspecific cross types. (A) Seed length and (B) length/width ratios. Violin plots show distribution of individual seeds. Letters indicate significance from post-hoc Tukey tests after running six independent species-pair models. One species pair had a significant reciprocal difference in hybrid seed size, while three pairs had a significant reciprocal difference in seed length/width ratio; length/width ratio was elevated compared to both parents for six cross types.

Table S1. Population location information and number of samples used per population.

					Samples used in crosses†		
Population	**Species**	**Latitude**	**Longitude**	**Samples sequenced**	**Seed families**	**1st gen**	**2nd gen**
J31	*M. johnstonii*	34.401950	-117.81580	5	4	9	7
B07	*M. brevipes*	34.358990	-118.39803	3	5	14	1
B11	*M. brevipes*	33.656155	-117.45298	6	5	13	7
B12	*M. brevipes*	32.889920	-116.57440	4	6	23	2
B19	*M. brevipes*	33.333300	-116.94200	4	6	33	20
F06	*M. fremontii*	34.693000	-119.32900	2	4	9	--
F21	*M. fremontii*	34.460560	-117.67316	3	4	11	--
F22	*M. fremontii*	34.376390	-117.59682	2	3	6	--
S25	'Sespe Creek'	34.565773	-119.26081	2	1	3	3
N01	*M. nanus*	42.638395	-118.57760	2	--	--	--
C01	*M. constrictus*	34.798960	-119.00466	1	--	--	--

† 1st gen = wild-collected, 2nd gen = greenhouse-produced from hand pollination. A
individuals were grown directly from wild-collected seeds, except the two *M. nan*
which were tissue collected from wild individuals.

Table S2. Sequencing and coverage information.

Sample info			Read pairs			Coverage per base	
Sample†	Pop	Batch	Raw	Aligned	%	All sites	% with >=4X coverage
BREV07_3_1	B07	1	47,522,461	13,277,523	27.9%	12.47	39.03%
BREV07_5_1	B07	1	49,800,600	15,174,402	30.5%	14.04	39.09%
BREV12_3_1	B12	1	49,704,577	15,840,128	31.9%	15.68	37.55%
BREV12_5_1	B12	1	49,785,466	14,465,999	29.1%	13.52	39.79%
BREV12_6_1	B19	1	49,555,797	15,518,193	31.3%	14.54	39.49%
BREV19_1_1	B19	1	49,652,489	16,050,274	32.3%	15.62	37.83%
FREM22_6_1	F22	1	49,332,251	8,451,160	17.1%	7.30	33.81%
JOHN31_5_1	J31	1	49,714,033	13,727,590	27.6%	12.82	37.51%
BREV07_6_1	B07	2	25,682,314	5,672,576	22.1%	5.67	32.30%
BREV11_5_3	B11	2	28,911,480	5,804,484	20.1%	5.35	31.82%
BREV12_4_1	B12	2	28,052,293	6,443,496	23.0%	6.28	33.38%
BREV19_2_1	B19	2	29,339,237	7,002,395	23.9%	6.87	33.83%
BREV19_3_1	B19	2	36,190,791	3,248,019	9.0%	3.10	21.10%
BREV19_4_1	B19	2	14,858,533	2,429,889	16.4%	2.19	16.18%
FREM06_3_2	F06	2	30,075,452	5,408,560	18.0%	4.51	26.45%
FREM06_4_3	F06	2	29,784,495	6,422,159	21.6%	5.68	29.74%
FREM21_2_1	F21	2	33,601,408	5,451,858	16.2%	4.60	27.10%
FREM22_5_1	F22	2	24,172,306	2,679,095	11.1%	2.35	19.37%
JOHN31_1_1	J31	2	47,347,007	6,441,313	13.6%	6.20	31.22%
JOHN31_2_1	J31	2	64,312,829	10,195,170	15.9%	9.88	36.43%
JOHN31_4_1	J31	2	23,147,570	3,938,270	17.0%	3.82	24.04%
JOHN31_5_2	J31	2	32,146,268	5,382,624	16.7%	4.86	25.48%
BREV11_1_11	B11	3	12,194,294	3,311,065	27.2%	3.16	18.64%
BREV11_3_4	B11	3	16,149,111	4,165,590	25.8%	3.88	24.46%
BREV11_5_1	B11	3	19,609,920	5,018,757	25.6%	4.72	26.70%
BREV11_6_11	B11	3	17,240,947	4,349,611	25.2%	4.02	26.63%
FREM21_3_11	F21	3	31,307,714	5,636,788	18.0%	4.86	30.25%
FREM21_4_11	F21	3	23,442,361	4,186,587	17.9%	3.67	24.90%
SESP25_1_1	S25	3	37,881,366	8,233,912	21.7%	7.70	34.70%
SESP25_1_2	S25	3	22,013,442	5,056,136	23.0%	4.58	29.93%
NANU01_1	N01	3	15,545,612	2,612,978	16.8%	2.26	14.32%
NANU01_2	N01	3	14,729,812	2,603,428	17.7%	2.38	17.61%

CONS01_1_1	C01	4	16,909,453	4,072,713	24.1%	4.10	16.6%
AURA_ari	AURA	SRX6077155	15,314,328	5,630,656	36.8%	7.14	64.06%
AURA_aur	AURA	SRX6077153	18,453,062	7,584,963	41.1%	10.02	75.92%
AURA_gra	AURA	SRX6077242	12,454,896	6,061,103	48.7%	7.84	66.98%
AURA_pun	AURA	SRX6077404	14,056,153	5,076,335	36.1%	6.53	60.90%
CLEV_cle	AURA	SRX6077240	12,810,520	4,567,552	35.7%	5.58	53.01%

† 1st number indicates population, 2nd number indicates maternal family, 3rd number refers to the individual plant. *M. nanus* samples (NANU01_1 and NANU01_2) are from distinct wild plants.

Table S3. Pedigree information for *M. brevipes* and *M. fremontii* F1 families.

				Number of individuals used		
Line name	Line type	Maternal	Paternal	Pollen viability	Maternal crosses	Paternal crosses
BF1	BxF F1 hybrid	B19_3_2	F6_4_3	0	1	1
BF2	BxF F1 hybrid	B12_5_2	F21_3_1	2	1	1
BF3	BxF F1 hybrid	B19_1_1	F6_3_1	7	7	6
BF5	BxF F1 hybrid	B19_4_14	F21_4_11	4	2	0

Table S4. Nucleotide diversity and divergence values at synonymous sites. Values were calculated using pixy for all individual pairwise comparisons, then averaged across comparisons within a group.

Species	Heterozygosity	Diversity
AUR	0.0025	0.0163
B	0.0198	0.0229
C	0.0135	--
F	0.0209	0.0316
J	0.0170	0.0174
N	0.0154	0.0324
S	0.0180	0.0178

Species 1	Species 2	Divergence
AUR	C	0.0940
AUR	N	0.0945
AUR	S	0.0991
AUR	B	0.1000
AUR	J	0.1005
AUR	F	0.1027
B	J	0.0525
B	F	0.0599

B	S	0.0697
B	C	0.0707
B	N	0.0830
C	S	0.0605
C	J	0.0702
C	F	0.0730
C	N	0.0753
F	J	0.0598
F	S	0.0715
F	N	0.0860
J	S	0.0692
J	N	0.0828
N	S	0.0791

Table S5. ABBA-BABA test results for the 'complete' SNP dataset.

P1	P2	P3	D	Z-score	Significance	*f4*-ratio	BBAA	ABBA	BABA
B	**J**	**F**	0.025	4.1	***	0.017	140199	101734	96787
B	**J**	**S**	0.077	14.5	***	0.023	225194	81493	69780
J	F	S	0.012	2.5	n.s.	0.004	193112	89515	87397
B	**F**	**S**	0.080	16.0	***	0.027	192818	93743	79920
B	**J**	**C**	0.060	12.4	***	0.015	217482	60440	53601
J	F	C	0.001	0.3	n.s.	0.000	190562	65810	65623
B	**F**	**C**	0.054	11.7	***	0.016	189827	68457	61448
C	**S**	**J**	0.193	38.6	***	0.072	128359	98268	66479
C	**S**	**F**	0.199	39.8	***	0.093	129273	101021	67419
C	**S**	**B**	0.186	35.9	***	0.077	133849	94966	65145
B	**J**	**N**	0.058	13.7	***	0.011	310955	59579	53098
F	**J**	**N**	0.027	8.0	***	0.006	281234	65746	62337
B	**F**	**N**	0.024	7.2	***	0.005	280189	64934	61873
J	**S**	**N**	0.091	24.8	***	0.027	184994	88233	73578
B	**S**	**N**	0.127	28.9	***	0.037	179236	92602	71726
F	**S**	**N**	0.110	28.9	***	0.032	190288	90971	73014
J	**C**	**N**	0.099	23.1	***	0.032	126808	82206	67332
B	**C**	**N**	0.131	25.7	***	0.042	124234	85599	65732
F	**C**	**N**	0.114	23.8	***	0.037	129720	84553	67229
S	**C**	**N**	0.036	7.9	***	0.010	166409	65159	60632

***p_{corr}<0.001, n.s.=not significant

Table S6. Crossing success and seed viability for each cross type.

Maternal species	Paternal species	Cross type	Crossing success (total crosses)	Seed viability (total seeds)
M. johnstonii	*M. johnstonii*	JxJ	0.538 (39)	0.745 (306)
M. johnstonii	*M. brevipes*	JxB	0.440 (25)	**0.000 (98)**
M. johnstonii	*M. fremontii*	JxF	0.600 (10)	**0.000 (78)**
M. johnstonii	Sespe Creek	JxS	0.600 (5)	**0.015 (66)**
M. brevipes	*M. johnstonii*	BxJ	0.484 (31)	**0.006 (630)**
M. brevipes	*M. brevipes*	BxB	0.902 (51)	0.981 (7292)
M. brevipes	*M. fremontii*	BxF	0.694 (36)	0.821 (2226)
M. brevipes	Sespe Creek	BxS	0.500 (6)	**0.018 (217)**
M. fremontii	*M. johnstonii*	FxJ	0.500 (20)	**0.012 (246)**
M. fremontii	*M. brevipes*	FxB	**0.017 (58)**	0.952 (21)
M. fremontii	*M. fremontii*	FxF	0.382 (55)	0.902 (911)
M. fremontii	Sespe Creek	FxS	0.091 (11)	**0.000 (8)**
Sespe Creek	*M. johnstonii*	SxJ	0.125 (8)	**0.000 (4)**
Sespe Creek	*M. brevipes*	SxB	0.333 (6)	**0.000 (38)**
Sespe Creek	*M. fremontii*	SxF	0.000 (4)	n/a (0)
Sespe Creek	Sespe Creek	SxS	0.409 (22)	0.909 (88)

Bolded values are significant in Tukey tests compared to both parental cross types.

Table S7. Average seed measurements and sample sizes by cross type.

Maternal species	Paternal species	Cross type	Seeds measured (number of fruits)	Average seed length (mm)	Average seed length/width ratio
M. johnstonii	*M. johnstonii*	JxJ	67 (7)	0.858	2.070
M. johnstonii	*M. brevipes*	JxB	50 (7)	0.865	4.729
M. johnstonii	*M. fremontii*	JxF	26 (3)	0.687	4.580
M. johnstonii	Sespe Creek	JxS	12 (1)	0.726	3.038
M. brevipes	*M. johnstonii*	BxJ	66 (5)	0.447	2.060
M. brevipes	*M. brevipes*	BxB	60 (4)	0.597	1.813
M. brevipes	*M. fremontii*	BxF	45 (3)	0.470	1.677
M. brevipes	Sespe Creek	BxS	56 (2)	0.523	2.155
M. fremontii	*M. johnstonii*	FxJ	9 (2)	0.579	2.901
M. fremontii	*M. brevipes*	FxB	15 (1)	0.584	1.989
M. fremontii	*M. fremontii*	FxF	27 (3)	0.641	2.149
M. fremontii	Sespe Creek	FxS	8 (1)	0.377	3.134

Sespe Creek	*M. johnstonii*	SxJ	22 (1)	0.415	3.274
Sespe Creek	*M. brevipes*	SxB	38 (2)	0.409	3.384
Sespe Creek	*M. fremontii*	SxF	15 (1)†	0.224†	2.965†
Sespe Creek	Sespe Creek	SxS	61 (6)	0.757	1.757

Bolded values are significant in Tukey tests compared to both parental cross types.
†Measured SxF 'seeds' were indistinguishable from unfertilized ovules.

Table S8. Pollen viability and counts with sample sizes.

Maternal species	Paternal species	Cross type	Average pollen viability (number of individuals) †	Pollen per unit area (number of individuals)
M. brevipes	*M. brevipes*	BxB	0.839 (13)	55.6 (13)
M. brevipes	*M. fremontii*	BxF	**0.235 (12)**	16.6 (13)
M. fremontii	*M. fremontii*	FxF	0.922 (8)	5.6 (10)

†excluding flowers with <10 counted pollen grains

Table S9. Statistical model structures and AIC values compared to null model equivalents.

Trait of interest	Model structure	Model type	AIC	AIC of null model †
Crossing success	Fruit_produced ~ Cross_type	BRGLM (Firth binomial)	**467.4**	576.2
Crossing success of BxF hybrids	Fruit_produced ~ Cross_type + (1 | Maternal_family)	GLMER (binomial)	**253.3**	291.7
Seed viability	cbind(viable_seeds,inviable_seeds) ~ Cross_type	BRGLM (Firth binomial)	**1566.2**	10533.6
Seed length (pure species only)	Length ~ Cross_type + (1 | Fruit)	LMER	**-600.8**	-598.5
Seed length (all cross types)	Length ~ Cross_type + (1 | Fruit)	LMER	-1131.6	-1141.3
Seed length/width ratio	Length/width ~ Cross_type + (1 | Fruit)	LMER	**1041.0**	1122.1
Pollen counts	round(Pollen_per_square) ~ Cross_type + (1 | Population)	GLMER (binomial)	**435.2**	438.2
Pollen viability	cbind(n_viable, n_inviable) ~ Cross_type + (1 | Population)	GLMER (binomial)	**491.0**	501.2
Female fertility	Seed_count ~ Cross_type	LM	**900.8**	913.5

†null model is the equivalent model excluding Cross_type as a model term.

REFERENCES

Aagaard, J. E., George, R. D., Fishman, L., MacCoss, M. J., & Swanson, W. J. (2013). Selection on Plant Male Function Genes Identifies Candidates for Reproductive Isolation of Yellow Monkeyflowers. *PLoS Genetics*, *9*(12). https://doi.org/10.1371/journal.pgen.1003965

Ascher, P. D., & Drewlow, L. W. (1975). The effect of prepollination injection with stigmatic exudate on interspecific pollen tube growth in Lilium longiflorum thunb. Styles. *Plant Science Letters*, *4*(6), 401–405. https://doi.org/10.1016/0304-4211(75)90269-2

Baack, E., Melo, M. C., Rieseberg, L. H., & Ortiz-Barrientos, D. (2015). The origins of reproductive isolation in plants. *New Phytologist*, *207*(4), 968–984. https://doi.org/10.1111/nph.13424

Baldwin, B. G., Goldman, D., Keil, D. J., Patterson, R., Rosatti, T. J., & Wilken, D. (Eds.). (2012). *The Jepson Manual: Vascular Plants of California, Thoroughly Revised and Expanded* (2nd ed.).

Barker, W. R. (Bill), Nesom, G. L., Beardsley, P. M., & Fraga, N. S. (2012). A taxonomic conspectus of phrymaceae: A narrowed circumscription for. *Phytoneuron*, *May*, 1–60.

Beardsley, P. M., Schoenig, S. E., Whittall, J. B., & Olmstead, R. G. (2004). Patterns of evolution in western North American Mimulus (Phrymaceae). *American Journal of Botany*, *91*(3), 474–489. https://doi.org/10.3732/ajb.91.3.474

Behm, J. E., Ives, A. R., & Boughman, J. W. (2010). Breakdown in postmating isolation and the collapse of a species pair through hybridization. *The American Naturalist*, *175*(1), 11–26. https://doi.org/10.1086/648559

Bernacchi, D., & Tanksley, S. D. (1997). An Interspecific Backcross of Lycopersicon esculentum × L. hirsutum: Linkage Analysis and a QTL Study of Sexual Compatibility Factors and Floral Traits. *Genetics*, *147*(2), 861–877. https://doi.org/10.1093/genetics/147.2.861

Bickford, D., Lohman, D. J., Sodhi, N. S., Ng, P. K. L., Meier, R., Winker, K., Ingram, K. K., & Das, I. (2007). Cryptic species as a window on diversity and conservation. *Trends in Ecology & Evolution*, *22*(3), 148–155. https://doi.org/10.1016/j.tree.2006.11.004

Bolger, A. M., Lohse, M., & Usadel, B. (2014). Trimmomatic: A flexible trimmer for Illumina sequence data. *Bioinformatics*, *30*(15), 2114–2120. https://doi.org/10.1093/bioinformatics/btu170

Bowers, J. E. (1982). The plant ecology of inland dunes in western North America. *Journal of Arid Environments*, *5*(3), 199–220. https://doi.org/10.1016/S0140-1963(18)31444-7

Brandvain, Y., & Haig, D. (2005). Divergent Mating Systems and Parental Conflict as a Barrier to Hybridization in Flowering Plants. *The American Naturalist*, *166*(3), 330–338. https://doi.org/10.1086/432036

Brandvain, Y., Kenney, A. M., Flagel, L., Coop, G., & Sweigart, A. L. (2014). Speciation and Introgression between Mimulus nasutus and Mimulus guttatus. *PLoS Genetics*, *10*(6), e1004410. https://doi.org/10.1371/journal.pgen.1004410

Broad Institute. (2019). *Picard Toolkit, GitHub repository*. https://broadinstitute.github.io/picard/

Christie, K., Fraser, L. S., & Lowry, D. B. (2022). The strength of reproductive isolating barriers in seed plants: Insights from studies quantifying premating and postmating reproductive barriers over the past 15 years. *Evolution*, evo.14565. https://doi.org/10.1111/evo.14565

Christie, K., & Strauss, S. Y. (2018). Along the speciation continuum: Quantifying intrinsic and extrinsic isolating barriers across five million years of evolutionary divergence in California jewelflowers. *Evolution*, *72*(5), 1063–1079. https://doi.org/10.1111/evo.13477

838 Coughlan, J. M., & Matute, D. R. (2020). The importance of intrinsic postzygotic barriers
839 throughout the speciation process: Intrinsic barriers throughout speciation.
840 *Philosophical Transactions of the Royal Society B: Biological Sciences*, *375*(1806).
841 https://doi.org/10.1098/rstb.2019.0533
842 Coughlan, J. M., Wilson Brown, M., & Willis, J. H. (2020). Patterns of Hybrid Seed Inviability in
843 the Mimulus guttatus sp. Complex Reveal a Potential Role of Parental Conflict in
844 Reproductive Isolation. *Current Biology*, *30*(1), 83-93.e5.
845 https://doi.org/10.1016/j.cub.2019.11.023
846 Coyne, J. A., & Orr, H. A. (1989). Patterns of Speciation in Drosophila. *Evolution*, *43*(2), 362–381.
847 Coyne, J. A., & Orr, H. A. (1997). Patterns of Speciation in Drosophila Revisited. *Evolution*, *51*(1),
848 295. https://doi.org/10.2307/2410984
849 Crespi, B., & Nosil, P. (2013). Conflictual speciation: Species formation via genomic conflict.
850 *Trends in Ecology & Evolution*, *28*(1), 48–57. https://doi.org/10.1016/j.tree.2012.08.015
851 Curtu, A. L., Gailing, O., & Finkeldey, R. (2009). Patterns of contemporary hybridization inferred
852 from paternity analysis in a four-oak-species forest. *BMC Evolutionary Biology*, *9*(1), 284.
853 https://doi.org/10.1186/1471-2148-9-284
854 Danecek, P., Bonfield, J. K., Liddle, J., Marshall, J., Ohan, V., Pollard, M. O., Whitwham, A.,
855 Keane, T., McCarthy, S. A., Davies, R. M., & Li, H. (2021). Twelve years of SAMtools and
856 BCFtools. *GigaScience*, *10*(2), giab008. https://doi.org/10.1093/gigascience/giab008
857 D'Angiolo, M., De Chiara, M., Yue, J.-X., Irizar, A., Stenberg, S., Persson, K., Llored, A., Barré, B.,
858 Schacherer, J., Marangoni, R., Gilson, E., Warringer, J., & Liti, G. (2020). A yeast living
859 ancestor reveals the origin of genomic introgressions. *Nature*, *587*(7834), Article 7834.
860 https://doi.org/10.1038/s41586-020-2889-1
861 Darwin, C. (1859). *On the origin of species by means of natural selection*. John Murray.
862 http://darwin-online.org.uk/converted/pdf/1861_OriginNY_F382.pdf
863 Ferris, K. G., Sexton, J. P., & Willis, J. H. (2014). Speciation on a local geographic scale: The
864 evolution of a rare rock outcrop specialist in *Mimulus*. *Philosophical Transactions of the*
865 *Royal Society B: Biological Sciences*, *369*(1648), 20140001.
866 https://doi.org/10.1098/rstb.2014.0001
867 Fishman, L. (2020). *96-well CTAB-chloroform DNA extraction*. protocols.io.
868 https://dx.doi.org/10.17504/protocols.io.bgv6jw9e
869 Fishman, L., Aagaard, J., & Tuthill, J. C. (2008). Toward the Evolutionary Genomics of
870 Gametophytic Divergence: Patterns of Transmission Ratio Distortion in Monkeyflower
871 (mimulus) Hybrids Reveal a Complex Genetic Basis for Conspecific Pollen Precedence.
872 *Evolution*, *62*(12), 2958–2970. https://doi.org/10.1111/j.1558-5646.2008.00475.x
873 Fishman, L., Sweigart, A. L., Kenney, A. M., & Campbell, S. (2014). Major quantitative trait loci
874 control divergence in critical photoperiod for flowering between selfing and outcrossing
875 species of monkeyflower (Mimulus). *New Phytologist*, *201*(4), 1498–1507.
876 https://doi.org/10.1111/nph.12618
877 Fishman, L., & Willis, J. H. (2006). A cytonuclear incompatibility causes anther sterility in
878 Mimulus hybrids. *Evolution*, *60*(7), 1372–1381. https://doi.org/10.1111/j.0014-
879 3820.2006.tb01216.x

Fitak, R. R. (2021). OptM: Estimating the optimal number of migration edges on population trees using Treemix. *Biology Methods and Protocols*, *6*(1), bpab017. https://doi.org/10.1093/biomethods/bpab017

Fujii, S., Tsuchimatsu, T., Kimura, Y., Ishida, S., Tangpranomkorn, S., Shimosato-Asano, H., Iwano, M., Furukawa, S., Itoyama, W., Wada, Y., Shimizu, K. K., & Takayama, S. (2019). A stigmatic gene confers interspecies incompatibility in the Brassicaceae. *Nature Plants*, *5*(7), Article 7. https://doi.org/10.1038/s41477-019-0444-6

GBIF.org. (2022). *GBIF Occurrence Download (12 September 2022).* https://doi.org/10.15468/dl.j8dxeq

Gore, P., Potts, B., Volker, P., & Megalos, J. (1990). Unilateral Cross-Incompatibility in Eucalyptus: The Case of Hybridisation Between E. globulus and E. nitens. *Australian Journal of Botany*, *38*(4), 383. https://doi.org/10.1071/BT9900383

Goulet, B. E., Roda, F., & Hopkins, R. (2017). Hybridization in plants: Old ideas, new techniques. *Plant Physiology*, *173*(1), 65–78. https://doi.org/10.1104/pp.16.01340

Grant, A. L. (1924). A Monograph of the Genus Mimulus. *Annals of the Missouri Botanical Garden*, *11*(2/3), 99–388. https://doi.org/10.2307/2394024

Grant, V. (1981). *Plant Speciation*. Columbia University Press.

Green, R. E., Krause, J., Briggs, A. W., Maricic, T., Stenzel, U., Kircher, M., Patterson, N., Li, H., Zhai, W., Fritz, M. H.-Y., Hansen, N. F., Durand, E. Y., Malaspinas, A.-S., Jensen, J. D., Marques-Bonet, T., Alkan, C., Prüfer, K., Meyer, M., Burbano, H. A., … Pääbo, S. (2010). A draft sequence of the Neandertal genome. *Science (New York, N.Y.)*, *328*(5979), 710–722. https://doi.org/10.1126/science.1188021

Guerrero, R. F., Muir, C. D., Josway, S., & Moyle, L. C. (2017). Pervasive antagonistic interactions among hybrid incompatibility loci. *PLOS Genetics*, *13*(6), e1006817. https://doi.org/10.1371/journal.pgen.1006817

Haig, D., & Westoby, M. (1991). Genomic imprinting in endosperm: Its effect on seed development in crosses between species, and between different ploidies of the same species, and its implications for the evolution of apomixis. *Philosophical Transactions - Royal Society of London, B*, *333*, 1–13.

Hamlin, J. A. P., Hibbins, M. S., & Moyle, L. C. (2020). Assessing biological factors affecting postspeciation introgression. *Evolution Letters*, *4*(2), 137–154. https://doi.org/10.1002/evl3.159

Hogenboom, N. G., Mather, K., Heslop-Harrison, J., & Lewis, D. (1975). Incompatibility and incongruity: Two different mechanisms for the non-functioning of intimate partner relationships. *Proceedings of the Royal Society of London. Series B. Biological Sciences*, *188*(1092), 361–375. https://doi.org/10.1098/rspb.1975.0025

Kay, K. M., Woolhouse, S., Smith, B. A., Pope, N. S., & Rajakaruna, N. (2018). Sympatric serpentine endemic Monardella (Lamiaceae) species maintain habitat differences despite hybridization. *Molecular Ecology*, *27*(9), 2302–2316. https://doi.org/10.1111/mec.14582

Kenney, A. M., & Sweigart, A. L. (2016). Reproductive isolation and introgression between sympatric Mimulus species. *Molecular Ecology*, *25*(11), 2499–2517. https://doi.org/10.1111/mec.13630

Kleindorfer, S., O'Connor, J. A., Dudaniec, R. Y., Myers, S. A., Robertson, J., & Sulloway, F. J. (2014). Species collapse via hybridization in Darwin's tree finches. *The American Naturalist*, *183*(3), 325–341. https://doi.org/10.1086/674899

Koch, M. A., Haubold, B., & Mitchell-Olds, T. (2000). Comparative Evolutionary Analysis of Chalcone Synthase and Alcohol Dehydrogenase Loci in Arabidopsis, Arabis, and Related Genera (Brassicaceae). *Molecular Biology and Evolution*, *17*(10), 1483–1498. https://doi.org/10.1093/oxfordjournals.molbev.a026248

Korunes, K. L., & Samuk, K. (2021). pixy: Unbiased estimation of nucleotide diversity and divergence in the presence of missing data. *Molecular Ecology Resources*, *21*(4), 1359–1368. https://doi.org/10.1111/1755-0998.13326

Kryvokhyzha, D. (n.d.). *GATK: The best practice for genotype calling in a non-model organism*. Dmytro Kryvokhyzha - Bioinformatics & Genomics Scientist. Retrieved August 8, 2022, from https://evodify.com/gatk-in-non-model-organism/

Kuboyama, T., Chung, C. S., & Takeda, G. (1994). The diversity of interspecific pollen-pistil incongruity in Nicotiana. *Sexual Plant Reproduction*, *7*(4), 250–258. https://doi.org/10.1007/BF00232744

Lafon-Placette, C., Johannessen, I. M., Hornslien, K. S., Ali, M. F., Bjerkan, K. N., Bramsiepe, J., Glöckle, B. M., Rebernig, C. A., Brysting, A. K., Grini, P. E., & Köhler, C. (2017). Endosperm-based hybridization barriers explain the pattern of gene flow between Arabidopsis lyrata and Arabidopsis arenosa in Central Europe. *Proceedings of the National Academy of Sciences*, *114*(6), E1027–E1035. https://doi.org/10.1073/pnas.1615123114

Lafon-Placette, C., & Köhler, C. (2016). Endosperm-based postzygotic hybridization barriers: Developmental mechanisms and evolutionary drivers. *Molecular Ecology*, *25*(11), 2620–2629. https://doi.org/10.1111/mec.13552

Le Gac, M., Hood, M. E., & Giraud, T. (2007). Evolution of Reproductive Isolation Within a Parasitic Fungal Species Complex. *Evolution*, *61*(7), 1781–1787. https://doi.org/10.1111/j.1558-5646.2007.00144.x

Leishman, M., Wright, I., Moles, A., & Westoby, M. (2000). The Evolutionary Ecology of Seed Size. *Seeds: The Ecology of Regeneration in Plant Communities*, *2*. https://doi.org/10.1079/9780851994321.0031

Li, H. (2018). *Seqtk* (1.3). https://github.com/lh3/seqtk

Li, H., & Durbin, R. (2009). Fast and accurate short read alignment with Burrows-Wheeler transform. *Bioinformatics*, *25*(14), 1754–1760. https://doi.org/10.1093/bioinformatics/btp324

Lowry, D. B., Sobel, J. M., Angert, A. L., Ashman, T.-L., Baker, R. L., Blackman, B. K., Brandvain, Y., Byers, K. J. R. P., Cooley, A. M., Coughlan, J. M., Dudash, M. R., Fenster, C. B., Ferris, K. G., Fishman, L., Friedman, J., Grossenbacher, D. L., Holeski, L. M., Ivey, C. T., Kay, K. M., … Yuan, Y.-W. (2019). The case for the continued use of the genus name Mimulus for all monkeyflowers. *TAXON*, *68*(4), 617–623. https://doi.org/10.1002/tax.12122

Lowry, D. B., & Willis, J. H. (2010). A widespread chromosomal inversion polymorphism contributes to a major life-history transition, local adaptation, and reproductive isolation. *PLoS Biology*, *8*(9). https://doi.org/10.1371/journal.pbio.1000500

Malinsky, M., Matschiner, M., & Svardal, H. (2021). Dsuite—Fast D-statistics and related admixture evidence from VCF files. *Molecular Ecology Resources*, *21*(2), 584–595. https://doi.org/10.1111/1755-0998.13265

Mallet, J., Beltrán, M., Neukirchen, W., & Linares, M. (2007). Natural hybridization in heliconiine butterflies: The species boundary as a continuum. *BMC Evolutionary Biology*, *7*(1), 28. https://doi.org/10.1186/1471-2148-7-28

Malone, J. H., & Fontenot, B. E. (2008). Patterns of Reproductive Isolation in Toads. *PLoS ONE*, *3*(12), e3900. https://doi.org/10.1371/journal.pone.0003900

Martin, S. H., & Van Belleghem, S. M. (2017). Exploring Evolutionary Relationships Across the Genome Using Topology Weighting. *Genetics*, *206*(1), 429–438. https://doi.org/10.1534/genetics.116.194720

Matute, D. R., & Cooper, B. S. (2021). Comparative studies on speciation: 30 years since Coyne and Orr. *Evolution*, *1989*, 1–15. https://doi.org/10.1111/evo.14181

Moyle, L. C., Olson, M. S., & Tiffin, P. (2004). Patterns of reproductive isolation in three angiosperm genera. *Evolution*, *58*(6), 1195–1208. https://doi.org/10.1111/j.0014-3820.2004.tb01700.x

Moyle, L. C., & Payseur, B. A. (2009). Reproductive isolation grows on trees. *Trends in Ecology & Evolution*, *24*(11), 591–598. https://doi.org/10.1016/j.tree.2009.05.010

Nelson, T. C., Stathos, A. M., Vanderpool, D. D., Finseth, F. R., Yuan, Y., & Fishman, L. (2021). Ancient and recent introgression shape the evolutionary history of pollinator adaptation and speciation in a model monkeyflower radiation (Mimulus section Erythranthe). *PLoS Genetics*, *17*(2), e1009095. https://doi.org/10.1371/journal.pgen.1009095

Nesom, G. L. (2013). Taxonomic notes on Diplacus (Phrymaceae). *Phytoneuron*, 8.

Oneal, E., Willis, J. H., & Franks, R. G. (2016). Disruption of endosperm development is a major cause of hybrid seed inviability between *Mimulus guttatus* and *Mimulus nudatus*. *New Phytologist*, *210*(3), 1107–1120. https://doi.org/10.1111/nph.13842

Pickrell, J. K., & Pritchard, J. K. (2012). Inference of Population Splits and Mixtures from Genome-Wide Allele Frequency Data. *PLOS Genetics*, *8*(11), e1002967. https://doi.org/10.1371/journal.pgen.1002967

Presgraves, D. C. (2002). Patterns of Postzygotic Isolation in Lepidoptera. *Evolution*, *56*(6), 1168–1183. https://doi.org/10.1111/j.0014-3820.2002.tb01430.x

Rabiee, M., Sayyari, E., & Mirarab, S. (2019). Multi-allele species reconstruction using ASTRAL. *Molecular Phylogenetics and Evolution*, *130*, 286–296. https://doi.org/10.1016/j.ympev.2018.10.033

Ramsey, J., Bradshaw, H. D., & Schemske, D. W. (2003). Components of reproductive isolation between the monkeyflowers Mimulus lewisii and M. cardinalis (Phrymaceae). *Evolution*, *57*(7), 1520–1534. https://doi.org/10.1111/j.0014-3820.2003.tb00360.x

Raunsgard, A., Opedal, Ø. H., Ekrem, R. K., Wright, J., Bolstad, G. H., Armbruster, W. S., & Pélabon, C. (2018). Intersexual conflict over seed size is stronger in more outcrossed populations of a mixed-mating plant. *Proceedings of the National Academy of Sciences*, *115*(45), 11561–11566. https://doi.org/10.1073/pnas.1810979115

Rebernig, C. A., Lafon-Placette, C., Hatorangan, M. R., Slotte, T., & Köhler, C. (2015). Non-reciprocal Interspecies Hybridization Barriers in the Capsella Genus Are Established in

the Endosperm. *PLOS Genetics*, *11*(6), e1005295. https://doi.org/10.1371/journal.pgen.1005295

Roda, F., & Hopkins, R. (2019). Correlated evolution of self and interspecific incompatibility across the range of a Texas wildflower. *New Phytologist*, *221*(1), 553–564. https://doi.org/10.1111/nph.15340

Roth, M., Florez-Rueda, A. M., & Städler, T. (2019). Differences in Effective Ploidy Drive Genome-Wide Endosperm Expression Polarization and Seed Failure in Wild Tomato Hybrids. *Genetics*, *212*(1), 141–152. https://doi.org/10.1534/genetics.119.302056

Rushworth, C. A., Wardlaw, A. M., Ross-Ibarra, J., & Brandvain, Y. (2022). Conflict over fertilization underlies the transient evolution of reinforcement. *PLOS Biology*, *20*(10), e3001814. https://doi.org/10.1371/journal.pbio.3001814

Sackton, T. (2022). *Natural selection constrains neutral diversity across a wide range of species* [R]. https://github.com/tsackton/linked-selection/blob/da62043544dce9c9342f0a393f41c63bec292fcf/misc_scripts/Identify_4D_Sites.pl (Original work published 2014)

Sandstedt, G. D., & Sweigart, A. L. (2022). Developmental evidence for parental conflict in driving Mimulus species barriers. *New Phytologist*, *236*(4), 1545–1557. https://doi.org/10.1111/nph.18438

Sandstedt, G. D., Wu, C. A., & Sweigart, A. L. (2020). Evolution of multiple postzygotic barriers between species of the Mimulus tilingii complex. *Evolution*, *75*, 600–613. https://doi.org/10.1111/evo.14105

Scascitelli, M., Whitney, K. D., Randell, R. A., King, M., Buerkle, C. A., & Rieseberg, L. H. (2010). Genome scan of hybridizing sunflowers from Texas (Helianthus annuus and H. debilis) reveals asymmetric patterns of introgression and small islands of genomic differentiation. *Molecular Ecology*, *19*(3), 521–541. https://doi.org/10.1111/j.1365-294X.2009.04504.x

Schliep, K. P. (2011). phangorn: Phylogenetic analysis in R. *Bioinformatics*, *27*(4), 592–593. https://doi.org/10.1093/bioinformatics/btq706

Schumer, M., Xu, C., Powell, D. L., Durvasula, A., Skov, L., Holland, C., Blazier, J. C., Sankararaman, S., Andolfatto, P., Gil, †, Rosenthal, G., & Przeworski, M. (2018). Natural selection interacts with recombination to shape the evolution of hybrid genomes. *Science*, *360*(6389), 656–660.

Schwarzbach, A. E., Donovan, L. A., & Rieseberg, L. H. (2001). Transgressive character expression in a hybrid sunflower species. *American Journal of Botany*, *88*(2), 270–277. https://doi.org/10.2307/2657018

Scopece, G., Musacchio, A., Widmer, A., & Cozzolino, S. (2007). Patterns of reproductive isolation in Mediterranean deceptive orchids. *Evolution*, *61*(11), 2623–2642. https://doi.org/10.1111/j.1558-5646.2007.00231.x

Servedio, M. R., & Hermisson, J. (2020). The evolution of partial reproductive isolation as an adaptive optimum. *Evolution*, *74*(1), 4–14. https://doi.org/10.1111/evo.13880

Skogsmyr, I., & Lankinen, Å. (2002). Sexual selection: An evolutionary force in plants? *Biological Reviews*, *77*(4), 537–562. https://doi.org/10.1017/S1464793102005973

1051 Sobel, J. M. (2010). *Speciation in the western North American wildflower genus Mimulus* [Ph.D.,
1052 Michigan State University].
1053 https://www.proquest.com/docview/873378456/abstract/950327CDE46D4690PQ/1
1054 Sobel, J. M. (2014). Ecogeographic Isolation and Speciation in the Genus Mimulus. *The*
1055 *American Naturalist*, *184*(5), 565–579. https://doi.org/10.1086/678235
1056 Sobel, J. M., & Chen, G. F. (2014). Unification of methods for estimating the strength of
1057 reproductive isolation. *Evolution*, *68*(5), 1511–1522. https://doi.org/10.1111/evo.12362
1058 Stamatakis, A. (2014). RAxML version 8: A tool for phylogenetic analysis and post-analysis of
1059 large phylogenies. *Bioinformatics*, *30*(9), 1312–1313.
1060 https://doi.org/10.1093/bioinformatics/btu033
1061 Stankowski, S., Chase, M. A., Fuiten, A. M., Rodrigues, M. F., Ralph, P. L., & Streisfeld, M. A.
1062 (2019). Widespread selection and gene flow shape the genomic landscape during a
1063 radiation of monkeyflowers. *PLOS Biology*, *17*(7), e3000391.
1064 https://doi.org/10.1371/journal.pbio.3000391
1065 Stathos, A., & Fishman, L. (2014). Chromosomal rearrangements directly cause underdominant
1066 F1 pollen sterility in Mimulus lewisii–Mimulus cardinalis hybrids. *Evolution*, *68*(11),
1067 3109–3119. https://doi.org/10.1111/evo.12503
1068 Streisfeld, M. A., & Kohn, J. R. (2005). Contrasting patterns of floral and molecular variation
1069 across a cline in Mimulus aurantiacus. *Evolution*, *59*(12), 2548–2559.
1070 https://doi.org/10.1111/j.0014-3820.2005.tb00968.x
1071 Streisfeld, M. A., & Rausher, M. D. (2009). Altered trans-Regulatory Control of Gene Expression
1072 in Multiple Anthocyanin Genes Contributes to Adaptive Flower Color Evolution in
1073 Mimulus aurantiacus. *Molecular Biology and Evolution*, *26*(2), 433–444.
1074 https://doi.org/10.1093/molbev/msn268
1075 Struck, T. H., Feder, J. L., Bendiksby, M., Birkeland, S., Cerca, J., Gusarov, V. I., Kistenich, S.,
1076 Larsson, K.-H., Liow, L. H., Nowak, M. D., Stedje, B., Bachmann, L., & Dimitrov, D. (2018).
1077 Finding Evolutionary Processes Hidden in Cryptic Species. *Trends in Ecology & Evolution*,
1078 *33*(3), 153–163. https://doi.org/10.1016/j.tree.2017.11.007
1079 Sweigart, A. L., Fishman, L., & Willis, J. H. (2006). A simple genetic incompatibility causes hybrid
1080 male sterility in mimulus. *Genetics*, *172*(4), 2465–2479.
1081 https://doi.org/10.1534/genetics.105.053686
1082 Takeuchi, H., & Higashiyama, T. (2012). A Species-Specific Cluster of Defensin-Like Genes
1083 Encodes Diffusible Pollen Tube Attractants in Arabidopsis. *PLOS Biology*, *10*(12),
1084 e1001449. https://doi.org/10.1371/journal.pbio.1001449
1085 Tovar-Méndez, A., Kumar, A., Kondo, K., Ashford, A., Baek, Y. S., Welch, L., Bedinger, P. A., &
1086 McClure, B. A. (2014). Restoring pistil-side self-incompatibility factors recapitulates an
1087 interspecific reproductive barrier between tomato species. *Plant Journal*, *77*(5), 727–
1088 736. https://doi.org/10.1111/tpj.12424
1089 Van der Auwera, G., & O'Connor, B. (2020). *Genomics in the Cloud: Using Docker, GATK, and*
1090 *WDL in Terra (1st Edition)*. O'Reilly Media.
1091 Wheeler, M. J., Franklin-Tong, V. E., & Franklin, F. C. H. (2001). The molecular and genetic basis
1092 of pollen–pistil interactions. *New Phytologist*, *151*(3), 565–584.
1093 https://doi.org/10.1046/j.0028-646x.2001.00229.x

Williams, E., & Rouse, J. (1988). Disparate Style Lengths Contribute to Isolation of Species in Rhododendron. *Australian Journal of Botany*, *36*(2), 183. https://doi.org/10.1071/BT9880183

Xiong, T., & Mallet, J. (2022). On the impermanence of species: The collapse of genetic incompatibilities in hybridizing populations. *Evolution*, *76*(11), 2498–2512. https://doi.org/10.1111/evo.14626

Yuan, Y.-W. (2019). Monkeyflowers (Mimulus): New model for plant developmental genetics and evo-devo. *New Phytologist*, *222*(2), 694–700. https://doi.org/10.1111/nph.15560

Yuan, Y.-W., Sagawa, J. M., Young, R. C., Christensen, B. J., & Bradshaw, H. D., Jr. (2013). Genetic Dissection of a Major Anthocyanin QTL Contributing to Pollinator-Mediated Reproductive Isolation Between Sister Species of Mimulus. *Genetics*, *194*(1), 255–263. https://doi.org/10.1534/genetics.112.146852

Zuellig, M. P., & Sweigart, A. L. (2018). A two-locus hybrid incompatibility is widespread, polymorphic, and active in natural populations of Mimulus. *Evolution*, *72*(11), 2394–2405. https://doi.org/10.1111/evo.13596